

THESIS FOR THE DEGREE OF DOCTOR OF PHILOSOPHY

Strategies to Reduce Gaseous KCl and Chlorine in  
Deposits during Combustion of Biomass  
in Fluidised Bed Boilers

HÅKAN KASSMAN

Department of Energy and Environment  
Division of Energy Technology  
CHALMERS UNIVERSITY OF TECHNOLOGY  
Göteborg, Sweden 2012

Strategies to Reduce Gaseous KCl and Chlorine in Deposits during  
Combustion of Biomass in Fluidised Bed Boilers

HÅKAN KASSMAN

ISBN 978-91-7385-667-6

© HÅKAN KASSMAN, 2012

Doktorsavhandlingar vid Chalmers tekniska högskola

Ny serie nr 3348

ISSN 0346-718X

Department of Energy and Environment

Division of Energy Technology

Chalmers University of Technology

SE-412 96 Göteborg

Sweden

Telephone +46 (0)31-772 1000

Reproservice, Chalmers University of Technology  
Göteborg, Sweden 2012

# Strategies to Reduce Gaseous KCl and Chlorine in Deposits during Combustion of Biomass in Fluidised Bed Boilers

HÅKAN KASSMAN

Department of Energy and Environment  
Chalmers University of Technology

## ABSTRACT

Combustion of a biomass with an enhanced content of alkali and chlorine (Cl) can result in operational problems including deposit formation and superheater corrosion. The strategies applied to reduce such problems include co-combustion and the use of additives. In this work, measures were investigated in order to decrease the risk of superheater corrosion by reducing gaseous KCl and the content of chlorine in deposits. The strategies applied were sulphation of KCl by sulphur/sulphate containing additives (i.e. elemental sulphur (S) and ammonium sulphate (AS)) and co-combustion with peat. Both sulphation of KCl and capture of potassium (K) in ash components can be of importance when peat is used. The experiments were mainly performed in a 12 MW circulation fluidised bed (CFB) boiler equipped for research purposes but also in a full-scale CFB boiler. The results were evaluated by means of IACM (on-line measurements of gaseous KCl), conventional gas analysis, deposit and corrosion probe measurements and ash analysis.

Ammonium sulphate performed significantly better than elemental sulphur. Thus the presence of SO<sub>3</sub> (i.e. AS) is of greater importance than that of SO<sub>2</sub> (i.e. S) for sulphation of gaseous KCl and reduction of chlorine in deposits. Only a minor reduction of gaseous KCl was obtained during co-combustion with peat although chlorine in the deposits was greatly reduced. This reduction was supposedly due to capture of K by reactive components from the peat ash in parallel to sulphation of KCl. These compounds remained unidentified. The effect of volatile combustibles on the sulphation of gaseous KCl was investigated. The poorest sulphation was attained during injection of ammonium sulphate in the upper part of the combustion chamber during the lowest air excess ratio. The explanation for this is that SO<sub>3</sub> was partly consumed by side reactions due to the presence of combustibles. These experimental results were supported by modelling, although the sulphation of KCl in the presence of combustibles were somewhat overestimated in the chemical kinetic model. Oxygen also had an effect on the sulphation when injecting AS in the cyclone. Less gaseous KCl was reduced during air excess ratio  $\lambda = 1.1$  compared to the higher air excess ratios. A correlation was also observed between the sulphation of gaseous KCl and reduced chlorine content in the deposits.

Keywords: *Sulphation, KCl, Combustion of biomass, Peat, Ammonium sulphate, IACM, Chlorine in deposits*



## List of Publications

This thesis is based on the work contained in the following publications, referred to by Roman numerals in the text:

- I. H. Kassman, M. Broström, M. Berg, L.-E. Åmand, Measures to Reduce Chlorine in Deposits: Application in a Large-Scale Circulating Fluidised Bed Boiler Firing Biomass, *Fuel* 90 (2011) 1325-1334.
- II. H. Kassman, L. Bäfver, L.-E. Åmand, The Importance of SO<sub>2</sub> and SO<sub>3</sub> for Sulphation of Gaseous KCl – An Experimental Investigation in a Biomass Fired CFB Boiler, *Combustion and Flame* 157 (2010) 1649-1657.
- III. H. Kassman, J. Pettersson, B.-M. Steenari, L.-E. Åmand, Two Strategies to Reduce Gaseous KCl and Chlorine in Deposits during Biomass Combustion - Injection of Ammonium Sulphate and Co-Combustion with Peat, *Fuel Processing Technology*. 10.1016/j.fuproc.2011.06.025 (2011).
- IV. H. Kassman, L.-E. Åmand, The Effect of Oxygen and Volatile Combustibles on the Sulphation of Gaseous KCl – An Experimental Approach, Submitted for publication (2011).
- V. H. Kassman, F. Normann, L.-E. Åmand, The Effect of Volatile Combustibles on the Sulphation of Gaseous KCl – A Modelling Approach, In manuscript.

Håkan Kassman is the principal author of all papers. Lars-Erik Åmand has been the main supervisor and has contributed to the content of all papers in discussions and text editing. The calculations in Paper V were carried out by Håkan Kassman and the results were evaluated together with Fredrik Normann. The other co-authors have all contributed in their individual areas of expertise in the papers.



## **Related publications not included in the thesis**

The following publications, although related to this thesis are not included.

### **Publications in peer-reviewed international scientific journals**

M. Broström, H. Kassman, A. Helgesson, M. Berg, C. Andersson, R. Backman, A. Nordin, Sulfation of corrosive alkali chlorides by ammonium sulfate in a biomass fired CFB boiler, *Fuel Processing Technology* 88 (2007) 1171-1177.

C. Forsberg, M. Broström, R. Backman, E. Edvardsson, S. Badiei, M. Berg, H. Kassman, Principle, calibration, and application of the in situ alkali chloride monitor, *Review of Scientific Instruments*, 80 (2009).

### **Publications in conference proceedings**

H. Kassman, C. Andersson, J. Högberg, L.-E. Åmand, K. Davidsson, Gas phase Alkali Chlorides and Deposits during Co-Combustion of Coal and Biomass, 19th International Conference on Fluidized Bed Combustion, Vienna, Austria, 2006.

K. Davidsson, L.-E. Åmand, H. Kassman, E. Edvardsson, J. Högberg, On-line Measurement of Alkali Chlorides during Co-Combustion of Coal and Biomass, 15th European Biomass Conference & Exhibition, Berlin, Germany, 2007.

H. Kassman, M. Holmgren, E. Edvardsson, L.-E. Åmand, J. Öhlin, Nitrogen Containing Additives for Simultaneous Reduction of KCl and NO<sub>x</sub> during Biomass Combustion in a CFB Boiler, 9th International Conference on Circulating Fluidized Beds, Hamburg, Germany, 2008.

H. Kassman, L. Båfver, L.-E. Åmand, Sulphation of Gaseous KCl in a Biomass Fired CFB Boiler, European Combustion Meeting, Vienna, Austria, 2009.

H. Kassman, J. Bohwalli, J. Pettersson, L.-E. Åmand, Ammonium Sulphate and Co-Combustion with Peat – Two Strategies to Reduce Gaseous KCl and Chlorine in Deposits during Biomass Combustion, Impacts of Fuel Quality, Lapland, Finland, 2010.

L.-E. Åmand, J. Öhlin, J. Bohwalli, H. Kassman, Primary Formation of PCDD/Fs in a Circulating Fluidized Bed Boiler Burning Biomass – Impacts of Fuel Quality, Impacts of Fuel Quality, Lapland, Finland, 2010.

H. Kassman, J. Öhlin, J. Bohwalli, L.-E. Åmand, Influence of O<sub>2</sub> during Sulphation of KCl in a Biomass Fired CFB Boiler, Swedish-Finnish Flame Days, Piteå, Sweden, 2011.





## **Acknowledgements**

First of all I would like to thank Associate Professor Lars-Erik Åmand for being an excellent supervisor and good friend. We have worked together for more than 20 years and it has always been a pleasure.

I'm grateful for the opportunity to present my thesis at the Department of Energy and Environment. The support provided by both my examiner Professor Filip Johnsson and Professor Henrik Thunman, the head of the Division of Energy Technology, is appreciated.

I would like to express my gratitude to Vattenfall AB for giving me the opportunity to work with my industrial PhD during the last three years.

I have had the pleasure of working with various co-authors in my papers. The contributions made to my thesis by Markus Broström, Magnus Berg, Linda Bäfver, Jesper Pettersson, Britt-Marie Steenari and Fredrik Normann are greatly appreciated.

Most of the experimental work was carried out in the CFB boiler at Kraftcentralen, Chalmers. The support from both the operating staff and the research engineers Rustan Marberg, Johannes Öhlin and Jessica Bohwalli has been very valuable.

I would also like to express my appreciation to all my colleagues at the Division of Energy Technology and at Vattenfall AB.

Finally, I would like to thank my wife Lisa for all the support during these years of hard work for both of us. To my four daughters Ella, Hanna, Nadja and Louise, perhaps this thesis will inspire you to take on challenges that may lie ahead.



## List of abbreviations and symbols

Alkali	Potassium (K) and sodium (Na)
KCl	The content of gaseous alkali chlorides is expressed as KCl
AS	Ammonium sulphate, (NH <sub>4</sub> ) <sub>2</sub> SO <sub>4</sub>
CFB	Circulating fluidised bed
DOAS	Differential optical absorption spectroscopy
FTIR	Fourier transformed infra-red
IACM	In-situ alkali chloride monitor
IC	Ion chromatography
ICP-OES	Inductive coupled plasma with optical emission spectroscopy
IR	Infra-red
LPI	Low-pressure impactor
MSS	Municipal sewage sludge
SEM-EDX	Scanning Electron Microscopy – Energy Dispersive X-ray
SNCR	Selective non-catalytic reduction
UV-VIS	Ultra violet - visible
XRD	X-ray diffraction
$\lambda$	Air excess ratio
$\tau$	Residence time



## Table of Contents

1	Introduction.....	3
1.1	Thesis objective.....	3
1.2	Content of the thesis.....	4
2	Ash-related problems during combustion.....	5
2.1	Strategies to reduce alkali related problems.....	7
2.2	Sulphation of KCl by sulphur/sulphate based additives.....	8
2.2.1	Interactions between SO <sub>2</sub> /SO <sub>3</sub> and the O/H radical pool.....	9
2.2.2	Modelling the fate of gaseous K, S, Cl.....	10
2.3	Co-combustion of biomass with peat.....	11
2.4	Pathways for KCl during combustion of biomass.....	13
3	Materials and methods.....	15
3.1	The research boiler at Chalmers.....	15
3.1.1	The test plans.....	16
3.1.2	Experimental parameters.....	17
3.2	Measurement techniques.....	18
3.2.1	IACM (In-situ Alkali Chloride Monitor).....	18
3.2.2	Gas analysis.....	19
3.2.3	Impactor.....	20
3.2.4	Deposit and initial corrosion.....	20
3.3	The measurement campaign in a full-scale CFB boiler.....	20
3.4	Modelling.....	22
4	KCl and flue gas chemistry.....	25
4.1	Transients, on-line fuel quality control.....	25
4.2	Importance of SO <sub>2</sub> /SO <sub>3</sub> on sulphation of gaseous KCl.....	26
4.3	Effect of oxygen and combustibles on sulphation of KCl.....	27
4.4	Modelling the effect of volatile combustibles.....	29
4.5	Summarised results concerning sulphation of gaseous KCl.....	31
5	Strategies to reduce KCl and chlorine in deposits.....	33
5.1	Sulphur/sulphate-based additives.....	33

5.1.1	Elemental sulphur and ammonium sulphate .....	33
5.1.2	Influence of O <sub>2</sub> on sulphation of KCl and chlorine in deposits .....	35
5.2	Ammonium sulphate and co-combustion of peat.....	38
5.3	Remarks concerning co-combustion with peat .....	41
6	The measurement campaign in Munksund .....	43
6.1	Results from the short-term measurements .....	43
6.2	Results from the long-term measurements.....	44
7	Conclusions.....	47
7.1	Importance of SO <sub>2</sub> and SO <sub>3</sub> for sulphation of gaseous KCl.....	47
7.2	Co-combustion and ammonium sulphate.....	48
7.3	Suggestions for future work .....	48
8	References.....	49

# 1 Introduction

Increasing energy consumption and global warming from greenhouse gases are a serious concern. Energy production from fossil fuels such as coal is an important source for greenhouse gases, among which carbon dioxide (CO<sub>2</sub>) has received most attention. The emission of greenhouse gases can be reduced by increasing the share of renewable energy sources (e.g. wind, solar, hydropower and geothermal energy) and biomass. Energy produced from biomass is not considered to contribute to the net CO<sub>2</sub> emissions to the atmosphere. Political actions have therefore been taken to increase the share of biomass utilisation as an alternative to fossil fuels.

This greater demand to utilise biomass for combustion means that a wider range of biomass fuels is now considered. During combustion significant variations are seen in the behaviour of for instance stem wood, demolition wood and annual biomasses such as straw. Their properties are related to certain parameters including: feeding properties; heating value; content of moisture; content of ash and volatiles. The composition of ash-forming elements can result in various operational problems during combustion. They are often described as alkali related problems and include slagging, fouling (deposit formation), high temperature corrosion and also bed agglomeration during fluidised bed combustion (FBC). The relation in a fuel mixture between alkali (potassium, K and sodium, Na), chlorine (Cl) and sulphur (S) has a great impact on such operational problems.

The content of alkali is generally high in biomass, and the chlorine content is also rather high in some biomass fuels. However, the content of sulphur is in general relatively low. Alkali (mainly K) released into the gas phase as alkali chlorides (expressed as KCl) can condense on cold surfaces such as superheater tubes. High levels of KCl in the flue gas often result in enhanced deposit formation while high content of KCl in deposits may accelerate superheater corrosion.

## 1.1 Thesis objective

The objective of this work is to improve the understanding of the behaviour of gaseous KCl during combustion of biomass and also evaluate strategies to reduce gaseous KCl and the content of chlorine in deposits. The strategies applied have been co-combustion of biomass with peat and addition of sulphur based additives (i.e. elemental sulphur and ammonium sulphate). The evaluation is based on results obtained from advanced measurement tools applied in full-scale measurement campaigns in fluidised bed boilers. The measurement tools applied included IACM which is a unique measurement device for gaseous alkali chlorides, conventional gas analysis, deposit and corrosion probes, and an impactor. Additionally, the gas phase chemistry focusing on KCl, SO<sub>3</sub> and SO<sub>2</sub> is investigated in a modelling approach based on the experimental results.

The focus has been on the following subjects:

- A comparison of sulphur (i.e.  $\text{SO}_2$ ) and ammonium sulphate (i.e.  $\text{SO}_3$ ) for sulphation of gaseous alkali chlorides and reduction of chlorine in deposits.
- An investigation into the effect of oxygen and volatile combustibles on the sulphation of gaseous KCl during injection of ammonium sulphate.
- A comparison of the experimental results concerning sulphation of KCl and the results obtained from a kinetic model.
- A comparison of the performance of co-combustion of peat and injection of ammonium sulphate as strategies to reduce gaseous KCl and reduction of chlorine in deposits.
- To establish whether the positive effects from peat are a result of alkali capture or of sulphation of the alkali chlorides or in fact from a combination of these two.

## **1.2 Content of the thesis**

This thesis consists of an introduction followed by five appended publications. The purpose with the introduction is to give a broader description of the subjects investigated in the publications and also summarise the work in the papers. The introduction consists of seven chapters.

Chapter 2 provides a background to the subject and presents various fuel or ash related challenges during biomass combustion. The focus is on measures for prevention of deposit formation and high temperature corrosion. Different approaches for modelling alkali chlorides in combustion are also described. Chapter 3 presents the experimental methods applied. Special attention is given to IACM, which is a unique measurement device for gaseous alkali chlorides.

Chapters 4 – 6 summarise the results in the appended papers. Chapter 4 treats gaseous KCl and the importance of  $\text{SO}_2$  or  $\text{SO}_3$  for sulphation of KCl. The effects of oxygen and volatile combustibles on the sulphation of gaseous KCl are presented. Chapter 5 deals with strategies for reduction of gaseous KCl and chlorine in deposits. These strategies were co-combustion of biomass with peat and addition of sulphur/sulphate based additives (i.e. ammonium sulphate and elemental sulphur). Chapter 6 summarises the results from a comparison between co-combustion of peat and injection of ammonium sulphate in a full-scale boiler. Finally, overall conclusions and suggestions for future work are presented in chapter 7.



## 2 Ash-related problems during combustion

Table 2.1 shows selected fuel properties from wood chips, wood pellets, straw pellets and two types of peat and coal respectively. These solid fuels can be divided into three parts: combustibles, moisture and ash forming matter. All elements except carbon (C), hydrogen (H), oxygen (O) and nitrogen (N) are potentially ash-forming [1]. The main ash-forming elements are silicon (Si), aluminium (Al), iron (Fe), calcium (Ca), magnesium (Mg), phosphorous, (P), potassium (K), sodium (Na), sulphur (S) and chlorine (Cl).

Operational problems arise in the presence of certain of these ash-forming elements during combustion of biomass. They are often described as alkali related problems and Table 2.1 shows that the concentration of alkali (K + Na) is significantly higher in ash from biomass (wood and straw) than it is in peat and coal. It is also observed that K is typically a factor 10 higher than Na. The higher ash content in peat and coal means that the alkali loading in mole/MWh can be significant. The chlorine content is also rather high in certain biomass fuels such as straw. The content of sulphur is, however, relatively low.

Potassium can be released by primary reactions during devolatilisation and by secondary reactions during char combustion [2]. K is mainly released into the gas phase as KCl and KOH during combustion of biomass, and KCl is dominant when the Cl content is high [2-6]. The presence of KOH in the gas phase is favoured at elevated temperatures, high content of water vapour (H<sub>2</sub>O) and low content of HCl [2, 4, 5]. Chlorine is mainly released as HCl or as metal chlorides such as KCl. K can condense on heat transferring surfaces (i.e. superheaters) as chlorides (KCl) and aerosol particles containing sulphates (K<sub>2</sub>SO<sub>4</sub>) can deposit as particles. High levels of KCl in the flue gas often result in enhanced deposit formation [7] while high content of KCl in deposits may accelerate superheater corrosion [8, 9].



**Fig. 2.1.** Agglomeration in the loop seal of a CFB boiler after operation with a fuel mix of 20% straw.



**Fig. 2.2.** Deposit formation on a superheater used in a grate fired boiler during combustion of waste wood.

Table 2.1. Selected fuel properties of biomass, peat and coal (Ref. Papers I, II, III, IV, and [10], [11]).

	Wood pellets <sup>a</sup>	Wood chips <sup>b</sup>	Straw pellets <sup>a</sup>	Bark <sup>c</sup>	Peat <sup>c</sup>	Peat <sup>d</sup>	Coal <sup>e</sup>	Coal <sup>f</sup>
Proximate analysis								
Water (wt-%, raw)	8.0	40.5	8.8	-	-	42	9.6	16.4
Ash (wt-%, dry)	0.3	0.9	5.6	2.2	3.2	4.1	9.8	10.3
Volatiles (wt-%, daf)	82	81.7	81.1	-	-	70	34.1	39.6
Ultimate analysis (wt-%, daf)								
C	50.5	50.0	49.3	52.5	54.7	56.9	81.7	79.9
H	6.1	6.0	6.2	5.8	5.9	6.1	4.8	5.4
O	43.3	43.7	43.4	39.1	36.9	34.0	11.1	12.4
S	<0.01	0.01	0.10	0.04	0.2	0.30	0.62	0.7
N	0.06	0.15	0.58	0.24	2.3	2.71	1.45	1.7
Cl	<0.01	0.01	0.30	0.03	0.03	0.04	0.32	0.02
Ash analysis (g/kg dry ash)								
K	97	128	110	37	4	3.6	13	17
Na	9	7	9	3	3	1.3	13	7
Al	8	5	6	18	26	77	81	97
Si	41	32	300	51	110	150	210	250
Fe	8	5	2	34	93	159	60	56
Ca	212	234	52	253	172	93	73	16
Mg	34	28	10	27	5	13	38	12
P	12	15	14	10	6	12	2	1
Lower heating value (MJ/kg)								
H, daf	18.9	18.7	18.4	18.4	21.0	21.9	31.9	31.9
H, raw	17.1	10.1	15.6	-	-	11.2	25.8	25.8

daf = dry and ash free, raw = as received, - = not analysed, a = paper II, b = paper IV, c = paper I, d = paper III, e = high chlorine bituminous coal from Poland in [10], f = low chlorine bituminous coal from South America in [11].

Fluidised bed combustion (FBC) of bio fuels rich in alkali and/or chlorine can result in bed agglomeration, deposit formation and high temperature corrosion [8, 12, 13]. The dominant mechanism for bed agglomeration is melt formation and it has been suggested that the coating layers formed on bed particles play an important role [14]. Mechanisms for deposit formation were reviewed [15] and an increased concentration of ash particles in the flue gas can cause increased deposit growth rate from impaction. Another important factor is the composition of the deposits. Sticky deposits can capture fly ash particles, which in turn increase the deposit growth rate. Increasing deposition rates

corresponded to higher levels of Cl and lower levels of S in the deposits for mixtures of peat and bark in an investigation by [7]. Fig. 2.1 shows agglomeration after three days of operation with a fuel mix consisting of wood pellets and 20 % straw in the loop seal of a circulating fluidised bed (CFB) boiler. Fig. 2.2 shows severe deposit formation on a superheater used in a grate fired boiler during combustion of waste wood rich in chlorine. Fig. 2.3 shows superheater corrosion under a deposit rich in chlorine from a tube located in a CFB boiler fired with waste wood. A simplified drawing of a tube and deposit with selected gas and ash components as well as corrosion products is also presented (Fig. 2.3).

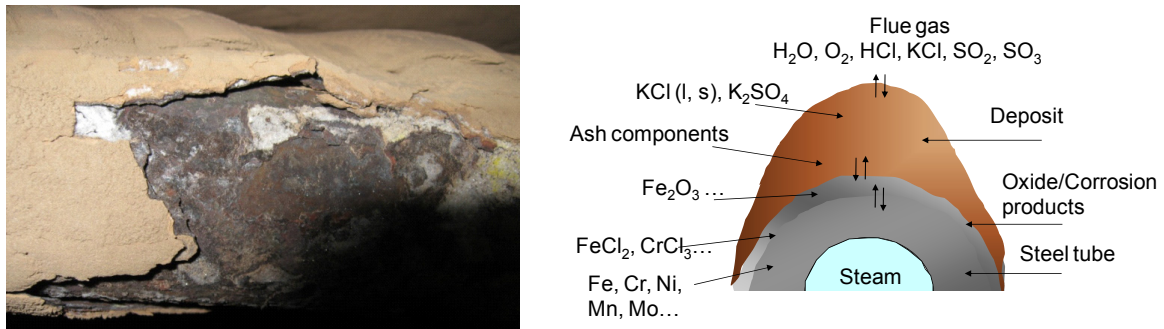


**Fig. 2.3.** Superheater corrosion under a deposit rich in chlorine from a tube located in a CFB boiler fired with waste wood. Simplified drawing of a tube and deposit with selected gas and ash components as well as corrosion products.

## 2.1 Strategies to reduce alkali related problems

Deposit formation and superheater corrosion can be mitigated by either co-combustion or the use of additives when firing biomass containing high amounts of alkali and chlorine. Coal, peat and municipal sewage sludge (MSS) are among the fuels used for co-combustion with biomass [16-18]. These measures can also have an impact on the bed agglomeration during combustion in fluidised bed boilers [19].

The chlorine content in the deposits can be reduced by means of both capture of K in ash components from the additional fuel, and/or sulphation of KCl due to its sulphur content. [16, 17, 20] [21-24]. The formation of alkali aluminosilicates was identified as the dominant path to capture alkali during co-combustion of coal and Meat and Bone Meal (MBM) [16]. In this investigation, sulphur in the different coals was less relevant in preventing alkali chloride deposition. The content of Cl in deposits was eliminated during co-combustion of a chlorine-rich biomass with MSS, whereas the content of K merely decreased [17]. The KCl concentration in the flue gas was partly limited by sulphation, and partly by capture of K by the sludge ash. K captured was found in species mainly composed of Si, Al, Ca, Fe and P. Especially important was the formation of potassium aluminium silicates, although the presence of Ca, Fe and P was also found to influence the alkali capture chemistry [25].

Additives can also capture K released during combustion in compounds, such as potassium aluminium silicates, thus preventing the formation of gaseous KCl. Additives used for the capture of K are for instance various clay minerals, including kaolin, the performance of which has been especially investigated [26-29]. Most of these additives have also been considered as sorbent materials for alkali for cleaning high temperature flue gases from pressurised fluidised bed combustors or for alkali removal in a biomass gasifier combined cycle application [30]. Sulphur/sulphate containing additives can be used for the sulphation of alkali chlorides and this is further discussed in Section 2.2.

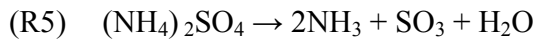
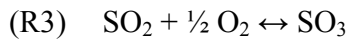
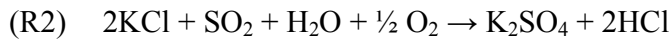
Another possibility to extend the lifetime of superheater tubes in a boiler is to replace low alloyed steels with more corrosion resistant materials. Chromia-forming austenitic stainless steels, high alloyed FeCr steels and Ni based superalloys are among the alternative materials when firing biomass and waste fuels. The low alloyed steels contain insufficient levels of chromium to form a protective chromia-rich oxide. Hence, low alloyed steels are poorly protected already from the outset. The increased corrosion rate in the presence of alkali chlorides in deposits is often attributed to the so-called active oxidation mechanism in which  $\text{Cl}_2(\text{g})$  acts as a catalyst in the corrosion attack [31]. Another mechanism based on the inward diffusion of chlorine ions has been proposed in recent years [32, 33]. However, it has been shown that even though more chromium-rich materials are being used, the corrosion rates remain unsatisfactorily high [34-37]. One reason for this has been suggested to be due to chromium depleting reactions between the deposit/flue gas and the protective oxide [34, 35]. Another process resulting in the breakdown of the protective oxide is the reaction between alkali salts (e.g. KCl, NaCl and  $\text{K}_2\text{CO}_3$ ) and the chromia-rich oxide forming chromate [32, 38].

## 2.2 Sulphation of KCl by sulphur/sulphate based additives

Elemental sulphur (S) or other sulphur/sulphate containing additives such as ammonium sulphate (AS,  $(\text{NH}_4)_2\text{SO}_4$ ) can be used for sulphation of alkali chlorides (mainly KCl during biomass combustion). Here the additive reacts with KCl, converting it to an alkali sulphate. In [39-42] results are presented from measurement campaigns in fluidised bed boilers when using elemental sulphur and/or ammonium sulphate.

Potassium can be released as KCl, or as KOH according to R1 when the concentration of water is high and that of chlorine is low [4]. Both homogeneous (gas phase) and heterogeneous (liquid or solid phase) mechanisms have been proposed for the formation of alkali sulphates from alkali chlorides found in deposits or in ash particles [43]. The homogeneous mechanism involves the formation of an alkali sulphate aerosol in the gas phase followed by nucleation and condensation onto a surface [43, 44]. Presented below is the overall sulphation reaction, R2, as well as other reactions (R3 – R5) of particular interest. The sulphur required in R2 can both originate from the fuel itself or from additives such as sulphur or ammonium sulphate. The sulphation rate in the gas phase is limited by the presence of sulphur trioxide ( $\text{SO}_3$ ) (R4) [6, 45-49] and oxidation of  $\text{SO}_2$  to  $\text{SO}_3$  (R3) is the rate-limiting step according to [6, 48-50].  $\text{SO}_2$  is formed when adding elemental sulphur and further oxidation to  $\text{SO}_3$  is required (R3). Below  $900^\circ\text{C}$  the oxidation of  $\text{SO}_2$  in R3 is slow. It can, however, be enhanced by radicals or be catalysed

by components in fly ash particles [48]. SO<sub>3</sub> is formed directly (R5) during injection of AS and the reaction (R4) between KCl and SO<sub>3</sub> takes place in the gas phase. According to R4, the sulphation of gaseous KCl is more efficient in the presence of SO<sub>3</sub> rather than SO<sub>2</sub>. The performance of elemental sulphur (i.e. SO<sub>2</sub>) and AS (i.e. SO<sub>3</sub>) for sulphation of gaseous KCl was evaluated in Paper II and AS lowered the concentration of gaseous KCl significantly better than sulphur. Thus, the presence of gaseous SO<sub>3</sub> was proven to be of greater importance than that of SO<sub>2</sub> for sulphation of gaseous KCl.

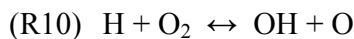
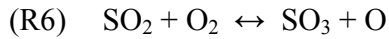


In a proposed heterogeneous mechanism, a gas phase alkali-containing precursor is transported to a surface where it is then sulphated by reactions in condensed or solid phases [43]. There is an efficient and fast heterogeneous formation mechanism for condensed phase alkali sulphates in flames that occurs on any surface including fly ash particles [51]. The heterogeneous mechanism is less important for the formation of alkali sulphate aerosols from gaseous alkali chlorides [48]. The rate of sulphation of KCl in gas phase and in condensed phases was investigated in [46], and found to be considerably slower in the condensed phase. Heterogeneous sulphation of KCl is of greater importance in deposits compared to particles in the flue gas, due to its longer reaction time. The investigations available concerning heterogeneous sulphation of alkali chlorides (R2) are rather old [46, 51, 52]. There are two mechanism presented in the literature for heterogeneous sulphation: Langmuir Hinselwood and Elay Rideal [53]. A simplified description without intermediates is that gaseous SO<sub>2</sub>, O<sub>2</sub> and H<sub>2</sub>O is adsorbed to an alkali chloride surface and SO<sub>3</sub> formed from the adsorbed species sulphate the alkali chloride.

### 2.2.1 Interactions between SO<sub>2</sub>/SO<sub>3</sub> and the O/H radical pool

There are interactions between the volatile combustibles and trace species including K, S, Cl and N during combustion [43]. CO is formed during oxidation of light volatile hydrocarbons such as methane. CO is further oxidised to CO<sub>2</sub> by a hydroxyl (OH) radical which is a part of the O/H radical pool. The radical pool is also involved in reactions with K, S, Cl and N. Calculations concerning the reactions of SO<sub>3</sub> with the O/H radical pool were presented in [54]. It was suggested that the oxidation of SO<sub>2</sub> to SO<sub>3</sub> involved recombination of SO<sub>2</sub> with oxygen (O) and OH radicals, and that the SO<sub>3</sub> concentration could be limited by hydrogen (H) radicals (R6 – R8). The reaction between SO<sub>3</sub> and hydrogen radicals (R8) is fast. The presence of H radicals can thus have a great influence on the efficiency during sulphation of gaseous KCl. The final oxidation of CO (R9) requires an OH radical and high concentrations of KCl can interact by inhibiting the CO oxidation [55]. The chain branching reaction (R10) is the most important reaction for radical production. The reaction with hydrocarbon radicals is normally faster than R9 and

R10 [56]. This leads to an accumulation of CO, which starts to oxidise when the hydrocarbon oxidation is completed. The effect of oxygen and volatile combustibles on the sulphation of gaseous KCl was investigated by an experimental approach in Paper IV.



## 2.2.2 Modelling the fate of gaseous K, S, Cl

Modelling of different processes in combustion poses a challenge and interactions between chemical reactions, fluid dynamics and heat transfer occur. Modelling to support experimental results concerning the fate of gaseous K, S and Cl during combustion are based on chemical reactions. These reactions can be treated using thermodynamic equilibrium calculations [57-60] and/or chemical kinetic models for gas phase interactions [48-50]. Becidan et al. [57] performed thermodynamic equilibrium calculations to study ammonium sulphate and a silica-based additive for reduction of corrosion in waste-fired boilers. Factsage was used in the calculations and it is based on minimisation of Gibbs free energy. Experiments concerning the release of K, Cl and S during pyrolysis and combustion of corn stover were supported with equilibrium calculations [59]. The limitations described include the uncertainty of whether equilibrium is reached for all species in real system due to slow kinetics, low temperatures or short residence times. The aim in [59] was to confirm trends qualitatively rather than to quantify species and distributions.

Glarborg and Marshall [50] presented a chemical kinetic model for the formation of gaseous alkali sulphates. The reaction mechanism consisted of subsets for  $\text{H}_2/\text{O}_2$  (O/H radical pool), alkali, sulphur and chlorine. The rate constants in the mechanism were mostly based on ab initio estimates of the thermodynamic properties for a number of intermediate species. In this model gaseous sulphation is initiated by the oxidation of  $\text{SO}_2$  to  $\text{SO}_3$ .  $\text{SO}_3$  recombines with either KCl to form potassium oxysulphur chloride ( $\text{KSO}_3\text{Cl}$ ) or with KOH to form potassium hydrogen sulphate ( $\text{KHSO}_4$ ), and they, in turn, form  $\text{K}_2\text{SO}_4$ . The reaction mechanisms were updated by Hindiyarti et al [49] concerning mainly  $\text{SO}_2$  oxidation chemistry and K/Cl/S interactions [54, 61, 62]. Modelling predictions were also carried out using a plug flow model and compared with experimental data from [44, 46-48]. The updated reaction mechanism is used in Paper V to model the effect of volatile combustibles on the sulphation of gaseous KCl based on the results presented in Paper IV.

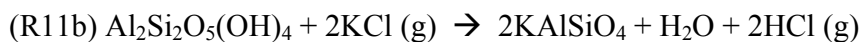
### 2.3 Co-combustion of biomass with peat

Co-combustion of biomass with peat can prevent bed agglomeration and reduce deposit formation and high temperature corrosion, when using biomass fuels rich in chlorine such as straw. During co-combustion with peat both sulphation of KCl due to the sulphur content in peat and capture of released K in peat ash minerals can be of importance.

Various peat fuels representing a wide range of ash-forming elements have been investigated [20, 21, 63]. Here the major ash-forming elements were Si, Al, Ca, Fe and S. The peat ashes consisted mainly of amorphous material and only small amounts of crystalline phases were detected by XRD (X-Ray Diffraction). The various peat types prevented bed agglomeration during co-combustion despite different compositions of ash-forming elements. The possible explanations in [21] included: reactions between alkali and sulphur to alkali sulphates; increased melting temperatures of bed particle layers due to increased content of Ca, Fe or Al; reaction of alkali and clay minerals to alkali aluminosilicates. The chemistry involved in bed agglomeration could also be relevant in a deposit or on fuel ash particles in the superheater region.

It was proposed in [21] that the positive effects on deposits during co-combustion with peat were capture of alkali in the gas phase to a less reactive particular form via reactive peat ash. The composition of the reactive components in the peat ash remained unidentified since only small amounts of crystalline phases were detected by XRD. Co-combustion of peat was one of the measures applied to reduce gaseous KCl and chlorine in the deposits during the large-scale investigation in Paper I. While only a minor reduction of gaseous KCl was obtained, the chlorine content in the deposits was greatly reduced. It remains unclear whether this reduction was due to heterogeneous sulphation or alkali capture on ash particles. Despite these efforts, the positive effects on deposit formation and superheater corrosion from peat are not yet fully understood.

Al and Si are among the major ash-forming elements in the peat ashes, and they could possibly capture alkali from alkali chlorides by means of formation of alkali aluminosilicates (KAl silicates). This formation is also important both during co-combustion with coal since its ash contains clay minerals [16, 24] and also during active addition of clay minerals such as pure kaolin [26-28]. Kaolin and several other aluminium silicates (bauxite, emathlite, diatomaceous earth) were among the sorbents for alkali in [30]. The main constituent of kaolin is kaolinite ( $\text{Al}_2\text{Si}_2\text{O}_5(\text{OH})_4$ ). The overall reactions between kaolinite and KCl in order to form KAl silicates (leucite ( $\text{KAlSi}_2\text{O}_6$ , R11a) and kalsilite ( $\text{KAlSiO}_4$ , R11b)) during release of HCl were presented by [26].



Sulphur in peat could sulphate an alkali chloride in the combustion chamber, in the flue gas and possibly also in a deposit according to (R2). The sulphation could, however, be affected by reactive calcium from the peat ash or from addition of limestone [22]. It was found that the chlorine content in deposits increased when the molar ratio  $\text{S}/(\text{Ca}+2\text{K}+2\text{Na})$  decreased during full-scale measurements. It was shown in [10] that both KCl (g) and Cl in the deposits increased during co-combustion of a chlorine-rich coal and biomass during addition of excess amounts of limestone.

The importance of the iron content for alkali capture is more difficult to establish. K captured during co-combustion of MSS and chlorine-rich biomass (straw) was found in species mainly composed of Si, Al, Ca, Fe and P [17, 25]. Phosphorous was also found together with Ca and Fe and possibly in the form of  $\text{KCa}_9\text{Fe}(\text{PO}_4)_7$  [17]. The Ca and Fe content in peat could thus be important in alkali capture chemistry. P and Ca can also capture alkali effectively [42, 64]. The slagging characteristics were investigated during combustion of cereal, rich in phosphorous and found that the formation of slag was reduced when Ca was added [65]. The reason for this was the formation of high-temperature melting calcium potassium phosphates (such as  $\text{CaKPO}_4$  and  $\text{Ca}_{10}\text{K}(\text{PO}_4)_7$ ) instead of low melting potassium phosphate ( $\text{KPO}_3$ ).

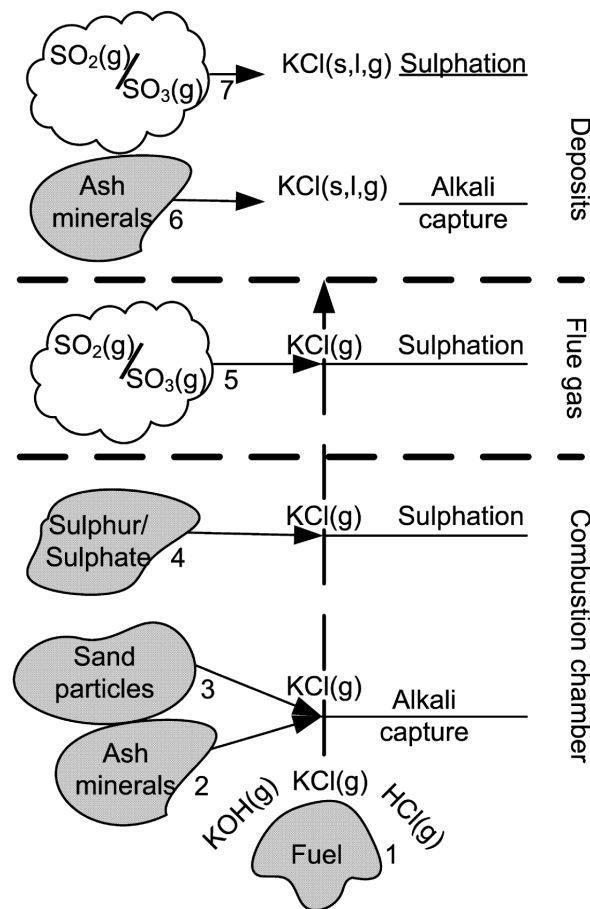


**Fig. 2.4.** Principal pathways for KCl during combustion of biomass. 1. Release of KOH, KCl, and HCl from a fuel particle; 2. Alkali capture by ash minerals (combustion chamber); 3. Alkali capture by reactions with sand particles; 4. Sulphation of KCl (combustion chamber); 5. Sulphation of gaseous KCl in the flue gas; 6. Alkali capture by ash minerals in deposits; 7. Sulphation of KCl (s,l) in deposits by  $\text{SO}_2/\text{SO}_3$ . Source Paper I.



## 2.4 Pathways for KCl during combustion of biomass

The principal pathways of K, Cl and S in a biomass fired boiler were described by [13]. [66] took a somewhat wider approach by including reactions between K and ash components such as aluminosilicates. Fig. 2.4 presents principal pathways for KCl during biomass combustion when applying the described strategies to reduce alkali related problems. During combustion of the fuel particles (1), KCl is either formed directly or from a reaction between KOH and HCl (R1). K from KCl may be captured in the combustion chamber by means of reactions with ash minerals (2), and sand particles (3). The ash minerals for alkali capture can originate from an additional fuel such as peat or an additive. KCl may also be sulphated (4) in the combustion chamber (R2). The sulphur can originate from an additional fuel or an additive such as elemental sulphur. Gaseous KCl present in the flue gas after the combustion chamber may be sulphated by  $\text{SO}_2(\text{g})/\text{SO}_3(\text{g})$  (5). The sulphation can either occur directly from  $\text{SO}_3$  by using ammonium sulphate (R4, R5) or after oxidation of  $\text{SO}_2$  from sulphur (R3). Sulphur in (R3) can, for instance, originate from peat or added elemental sulphur. KCl (s, l) condensed in deposits is undesirable, since deposits rich in chlorine may cause enhanced corrosion of superheater tubes [8]. Capture of K (6) by ash minerals such as in reactions R11a and R11b during release of HCl may also render the deposit less corrosive. Heterogeneous sulphation by  $\text{SO}_2(\text{g})/\text{SO}_3(\text{g})$  (7) according to R2 can also occur.



### 3 Materials and methods

The experiments in Papers II, III and IV were performed in a 12 MW CFB boiler equipped for research purposes. The modelling in Paper V was based on results obtained in Paper IV. The experimental methods in these papers are further described in Sections 3.1, 3.2 and 3.4. The experiments in Paper I were carried out in a full-scale boiler and the methods applied are discussed in Section 3.3.

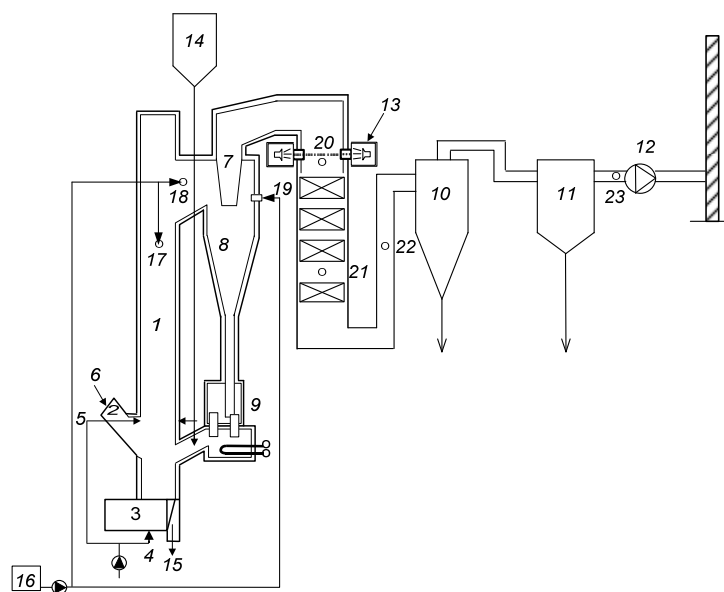


**Fig. 3.1.** The 12 MW CFB boiler. 1. furnace; 2. fuel chute; 3. air plenum; 4. primary air; 5. secondary air; 6. fuel feed and sand; 7. cyclone outlet; 8. primary cyclone; 9. particle seal; 10. secondary cyclone; 11. bag house filter; 12. flue gas fan; 13. IACM (*In-situ* Alkali Chloride Monitor); 14. Sulphur (Paper I), PVC and kaolin (Paper III), kaolin (paper IV); 15. bed material; 16. ammonium sulphate (AS); 17-19. injection of AS and measurement positions; 17. upper part of the combustion chamber; 18 cyclone inlet; 19. in the cyclone; 20-23. measurement positions; 20. before the convection pass; 21. in the convection pass (LPI), 22. after the convection pass; 23. before the stack.

#### 3.1 The research boiler at Chalmers

The experiments in Papers II, III and IV were performed in the 12 MW CFB boiler at Chalmers University of Technology shown in Fig. 3.1. This boiler is mainly used for research purposes and it offers the possibility to perform measurement campaigns in a full-scale boiler, while maintaining control over important operational parameters such as load, air supply and composition of the fuel mix. The boiler has been described earlier in several publications including [10, 17, 19, 41]. The combustion chamber has a square cross-section of approximately  $2.25 \text{ m}^2$  and a height of 13.6 m. Fuel is fed from a fuel

chute (located at the front of the boiler) to the lower part of the combustion chamber. The bed material is recirculated through the cyclone back to the combustion chamber. Meanwhile the combustion gases enter the convection pass where the gases are cooled down to 150°C before cleaning in a secondary cyclone and a bag house filter. Operating conditions typical of CFB boilers were selected and are presented in the corresponding Papers. The base fuel was wood pellets/wood chips and straw pellets were used as additional fuel with a constant ratio of about 20 - 30% of the energy input to the boiler to increase the level of gaseous KCl. Co-combustion was also carried out in Paper III with a mixture of straw pellets and peat. The peat selected had a rather low calcium content and the major ash-forming elements were Al, Fe, Ca, Si and S. Fuel properties are presented in Table 2.1.

### 3.1.1 The test plans

In Paper II, elemental sulphur (S) and ammonium sulphate (AS) were added at the different molar ratios of S/Cl. The lowest molar ratios (AS1, S1) were at 2.1 and the highest ones were 5.1 (AS3) and 6.4 (S3). Sulphur was introduced to the lower part of the combustion chamber through the return leg from the hot cyclone (14 in Fig 3.1) whereas AS was added before the primary cyclone (18).

The test plan in Paper III consisted of four main test cases: Ref, Peat, RefCl and ASCl. The reference case (Ref) was wood pellets with straw pellets at a constant ratio of about 25% of the energy input. During co-combustion of peat (test case Peat), a mixture of straw pellets and peat was used to obtain similar molar flows of alkali and chlorine as in Ref, and this also resulted in higher molar flows of Al and Fe. A flue gas with a further enhanced level of KCl (RefCl) was achieved by adding polyvinyl chloride (PVC) to (14) in Fig 3.1. Ammonium sulphate was added in a location before the primary cyclone (18). The conditions here were similar to those during RefCl and the test case was named ASCl. The molar flow of chlorine was high in RefCl and ASCl.

The measurements in Paper IV were carried out during three air excess ratios ( $\lambda = 1.1, 1.2$  and  $1.4$ ). Ammonium sulphate was injected into the boiler according to two experimental procedures. The first procedure, a so-called “transient test”, was carried out for the three excess air ratios. Increasing amounts of AS were injected in a sequence at three positions. They were in the upper part of the combustion chamber (17 in Fig. 3.1), in the cyclone inlet (18) and in the cyclone (19). Each sequence consisted of a reference (Ref) and injection of increasing amounts of AS (i.e. molar ratios of S/Cl) and was performed for 25 minutes. In the second experimental procedure, AS was injected into the cyclone at three air excess ratios. Each measurement was carried out for three hours and several measurement tools were applied including IACM, deposit probes and conventional gas analysis. The measurements were performed for a reference case (Ref) and two flows of AS (low flow (amount) of AS = ASL, high flow = ASH).

### 3.1.2 Experimental parameters

The performance of ammonium sulphate and elemental sulphur was evaluated by using certain experimental parameters. The ability of peat to capture alkali and/or sulphate KCl was evaluated by an extended amount of experimental parameters. These parameters were either molar ratios or molar flows of certain elements as shown in Table 3.1 (Ref. Paper III). The importance of the experimental parameters focusing on Paper III is discussed briefly and more details can be found in the corresponding papers.

Table 3.1. Experimental parameters – molar flows and molar ratios (Source Paper III).

Test case	Ref	Peat	RefCl	ASCl
Molar flows (mol/MWh)				
Alkali (Na+K)	13.5	14.0	11.9	15.5
Chlorine (Cl)	5.1	5.7	10.2	10.1
Sulphur (S)	1.9	10.7	1.7	10.6
Aluminium (Al)	0.5	12.6	0.5	0.6
Iron (Fe)	0.2	12.6	0.2	0.3
Calcium (Ca)	6.4	16.0	6.0	8.4
Molar ratios (mol/mol)				
S/Cl	0.38	1.89	0.17	1.05
S/(Ca+2K+2Na)	0.06	0.24	0.06	0.27
Cl/(K+Na)	0.38	0.40	0.86	0.65
Ca/S	3.3	1.5	3.6	0.8
Al/K+Na	0.04	0.92	0.04	0.04

The molar ratio S/Cl is a measure to what extent a fuel mix is corrosive and is presented here for the total amount of sulphur in both the fuel and the additive. Theoretically, a molar ratio of 0.5 is sufficient to produce  $K_2SO_4$  if K prefers S over Cl. In practice, however, S and Cl compete with each other and an excess of S is needed to prevent the formation of KCl. The risk of corrosion was considered great at a molar ratio S/Cl less than 2.0, yet low at an S/Cl above 4.0 [67]. The chlorine content in the deposits is also a measure of the risk of corrosion. No chlorine was found when sulphur was available in the form of  $SO_3$  (i.e. ammonium sulphate) instead of  $SO_2$  at a molar ratio S/Cl of 2.1 in Paper II and 1.0 in Paper III. Thus the form of oxidised sulphur (i.e.  $SO_2$  or  $SO_3$ ) has an impact on the risk of corrosion. Calcium in the fuel ash is reactive and it also competes with potassium in reacting with sulphur and chlorine. The molar flow of Ca was significantly higher during test case Peat. During co-combustion of biomass with peat and coal, Cl in the deposits increased at molar ratios of S/(Ca+2K+2Na) lower than 0.2 in the fuel [22]. Sulphur can both originate from the fuel and the additive in the molar ratios S/(Ca+2K+2Na) and Ca/S in Table 3.1. The molar ratio Cl/(K+Na) is a measure of the amount of Cl available in relation to the alkali content of the fuel. This ratio varied

between 0.4 and 0.9 for the present test cases, suggesting insufficient Cl present to form KCl from all K in the fuel even during the case RefCl. As expected, the sulphur input load varied significantly, since most of the sulphur originated from the peat or ammonium sulphate. The Al, Fe and Ca input load was high for Peat and especially aluminium containing minerals are known to be involved in alkali capture reactions.

## 3.2 Measurement techniques

Several advanced measurement and analytical techniques have been applied such as IACM, conventional gas analysis, deposit and corrosion measurements followed by analysis of collected deposits and exposed materials, and impactor measurements.

### 3.2.1 IACM (In-situ Alkali Chloride Monitor)

A so-called IACM (In-situ Alkali Chloride Monitor) located at (13) in Fig. 3.1 was used to measure the alkali chlorides in the gas phase [68, 69]. The IACM instrument measures the sum of the KCl and NaCl concentrations on-line but can not distinguish between these two species. IACM measures no other gaseous alkali species such as KOH (g). There is a higher content of K in relation to Na in biomass (Table 2.1). The result is expressed as KCl during combustion of biomass since it is the dominant gaseous alkali chloride at conditions prevailing in for instance a CFB boiler [5]. IACM also measures SO<sub>2</sub> simultaneously.

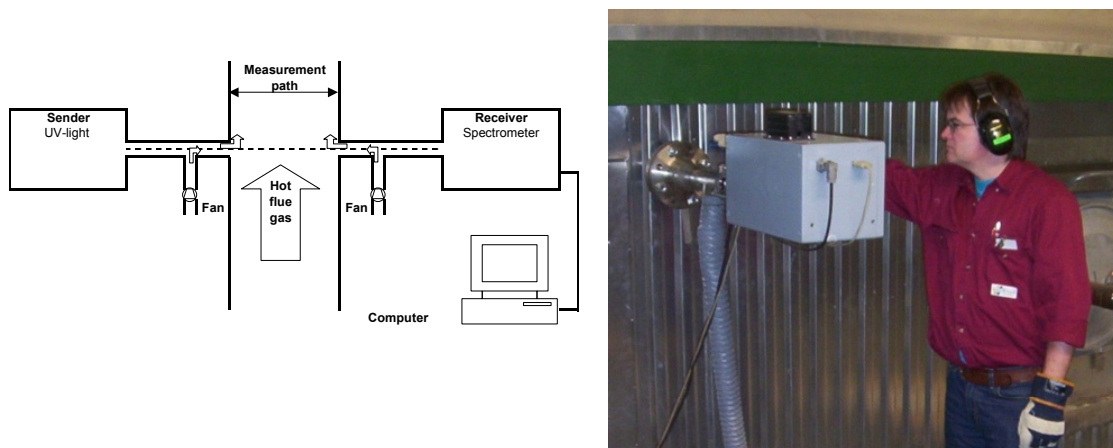


**Fig. 3.2.** Schematic view of an IACM installation. The receiver side of an IACM installation.

A schematic view of IACM and a photograph of the receiver side from an installation are shown in Fig. 3.2. Light from a xenon lamp is sent across the furnace or flue gas channel (measurement path). The light, which arrives at the receiver, is analysed by a spectrometer. The measuring principle is based on molecular absorption at characteristic wavelengths in the Ultra Violet (UV) - visible region (VIS). The evaluation is made by

means of Differential Optical Absorption Spectroscopy (DOAS) and is described in more detail in [68]. The absorption patterns of  $\text{KCl(g)} + \text{NaCl(g)}$  are similar and located in the same wavelength region and it is difficult to differentiate between them due to spectral overlap. Fig. 3.3 shows absorption cross-sections of the components measured with IACM at  $860^\circ\text{C}$  [68]. The detection limit at a measuring length of 5 metres is 1 ppm for  $\text{KCl}$  and  $\text{NaCl}$  and 4 ppm for  $\text{SO}_2$  respectively. IACM has been used in the present boiler in several previous projects related to alkali chloride issues [10, 17, 19, 41]. IACM is a part of the ChlorOut concept. It consists of IACM and a sulphate-containing additive that converts alkali chlorides to less corrosive alkali sulphates [69, 70]. The sulphate-containing additive is often ammonium sulphate, although other sulphates are included in the ChlorOut concept as well. A particular advantage with ammonium sulphate is that a significant  $\text{NO}_x$  reduction is achieved parallel to the sulphation of alkali chlorides [41].

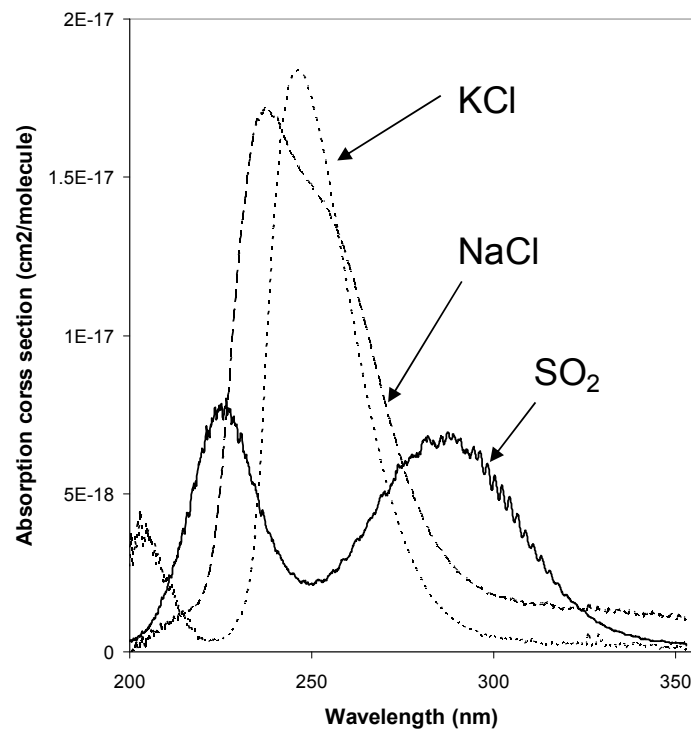


**Fig. 3.3.** Absorption cross-sections of the components measured with the IACM at  $860^\circ\text{C}$ .  $\text{KCl}$ ,  $\text{NaCl}$  and  $\text{SO}_2$  are represented by a dotted, dashed and solid line respectively.

### 3.2.2 Gas analysis

Flue gas was extracted through a heated probe and heated sampling lines to an FTIR (Fourier Transform Infra-Red) analyser for the determination of  $\text{HCl}$ ,  $\text{SO}_2$ ,  $\text{H}_2\text{O}$ ,  $\text{N}_2\text{O}$ ,  $\text{NO}$ ,  $\text{NO}_2$  and  $\text{NH}_3$  on hot wet flue gases. The flue gas was further transported to on-line IR-VIS instruments measuring  $\text{CO}$  and  $\text{SO}_2$  on cold dry gases and a paramagnetic analyser for  $\text{O}_2$ . A chemiluminescence analyser was used for  $\text{NO}$  and a flame ionisation

detector (FID) for volatile hydrocarbons ( $HC_{tot}$ ) in connection to the cold system. Methane ( $CH_4$ ) was used for calibration of the FID analyser and consequently  $HC_{tot}$  is presented as ppm methane equivalents. Gas concentrations were measured in locations after the convection path (22) and before the stack (23) during all test cases. Additional gas measurements were also carried out during the transient tests in Paper IV to characterise the composition of the flue gas at measurement locations (17), (18), (19), (20), (22) and (23) in Fig. 3.1.

### 3.2.3 Impactor

The sampling location for particles was in the convection pass (20 in Fig 3.1) before the economiser at a flue gas temperature of approximately 270°C. The sampling procedure is described in more detail in Papers I, III and [71]. Flue gas was isokinetically sampled through a heated probe followed by a pre-cyclone for collection of larger particles. A Dekati Low-Pressure Impactor (LPI) was used for the measurement of concentration and mass size distribution of particles ranging from 10  $\mu m$  down to 30 nm. The LPI was equipped with 13 stages representing a specific particle size range and the particles were separated according to their aerodynamic diameter. After sampling, the substrates were analysed with respect to chlorides (Cl) and sulphates ( $SO_4^{2-}$ ) using IC (Ion Chromatography) and K, Na, Ca, Mg, P, Al, Fe, Ba, Mn and Si using ICP-OES (Inductive Coupled Plasma with Optical Emission Spectroscopy).

### 3.2.4 Deposit and initial corrosion

The deposit and corrosion measurements were carried out before the convection pass (20 in Fig. 3.1) using temperature controlled probes. The measurements were carried out in similar ways in Papers I, III and IV and a brief description of the procedure in Paper III is given below. Steel rings were exposed for 4 hours at 500°C and 600°C material temperature, respectively. The ring materials were 304L and Sanicro 28, and the focus during evaluation was on the composition of deposits collected and initial corrosion. The sample rings exposed were either analysed quantitatively by means of wet chemistry or qualitatively by deposit and corrosion analysis. The quantitative analysis included ICP-OES and IC, whereas the qualitative analysis included Scanning Electron Microscopy – Energy Dispersive X-ray (SEM-EDX) and X-Ray Diffraction (XRD). These analytical methods provided different kinds of information which enabled a more detailed evaluation of the characteristics of the deposits collected. SEM-EDX and XRD analysis were performed on the windward side of the rings, whereas the ICP-OES and IC analyses were made on all of the deposits on the ring.

## 3.3 The measurement campaign in a full-scale CFB boiler

Most experiments in the thesis were carried out in the research boiler at Chalmers. Results from such well-controlled measurements should also be verified in larger commercial boilers. The performance and evaluation of measurement campaigns in full-



scale boilers pose a real challenge. Often identical operating conditions can not be achieved from one day to the next rendering the interpretation of the results more difficult. Full-scale measurements focusing on operational problems during biomass combustion have often been carried out involving researchers from Sweden, Denmark and Finland [22, 39, 42, 64, 72]. The Danish findings concerning ash formation, deposition and corrosion during straw utilisation were recently summarised by Frandsen [73].

The experiments in Paper I were performed in a full-scale CFB boiler of Foster Wheeler design situated in Munksund in northern Sweden. This boiler has a total production capacity of 96MW, of which 25MW can be produced as electricity. The load can vary significantly since the boiler provides process steam to a pulp and paper mill. At the time of the project, the boiler was mainly fired with bark (> 80 %), although sawdust, forest residues, and a chlorine containing plastic waste (reject) were also used. The scope was to demonstrate measures to reduce alkali related problems in a large-scale boiler. The measures applied were sulphation of KCl by ammonium sulphate and co-combustion with peat. These tests were included in a larger project and some of the results mainly focusing on other aspects have been presented previously [40, 74].

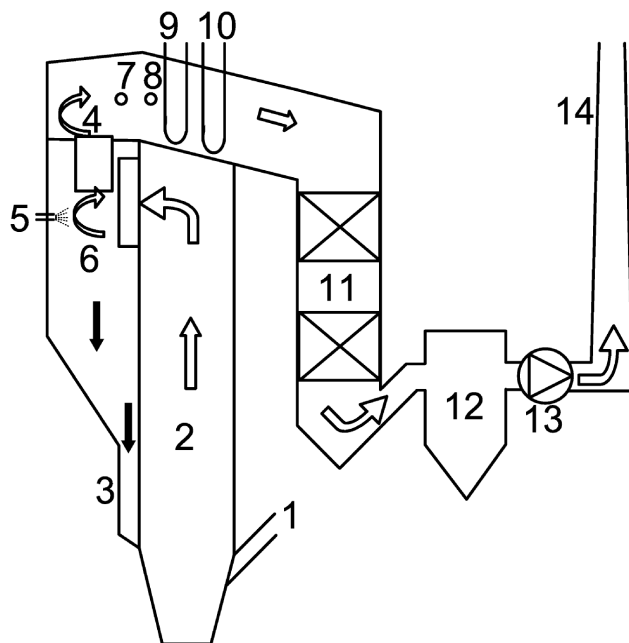


**Fig. 3.4.** Sketch of the CFB boiler. 1. fuel feed and sand; 2. furnace; 3. primary cyclone; 4. loop seal; 5. injection point of ammonium sulphate; 6. cyclone outlet; 7. IACM; 8. deposit probe, impactor; 9. superheater SH2 (13CrMo44); 10. superheater SH1 (15Mo3); 11. convection pass; 12. electrostatic precipitator; 13. flue gas fan; 14. stack.

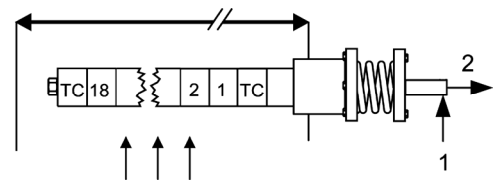


**Fig. 3.5.** The corrosion probe. 1. inlet cooling air; 2. outlet cooling air. The material and positions (pos) for the test rings on the were: 15Mo3 pos 1, 4, 7, 10; 10CrMo910 pos 2, 5, 8, 13, 15; 13CrMo44 pos 3, 6, 9, 11, 14, 16; X20 pos 12, 18; and Esshete 1250 pos 17.

The main test plan consisted of short-term measurements during three test cases: a reference case with normal fuel mix (Ref); normal fuel mix and injection of ammonium

sulphate (AS); co-combustion with approximately 20% peat on energy basis (Peat). The chemical composition of the flue gas in the superheater region was characterised by means of IACM and deposit measurements during the short-term campaign. These measurements were evaluated together with data from an FTIR and from the data recording system of the plant concerning stack emissions and operating conditions. Additional impactor measurements provided information about mass size distributions of extracted particles and the composition of elements in these size distributions. Further details concerning the experimental strategy can be found in Paper I.

Long-term measurements were carried out for test cases AS and Ref and the focus of these measurements was superheater corrosion. The boiler, Fig. 3.4, has two parallel cyclones which split the flue gases into two separate streams until they are mixed again prior to the first superheater (SH2). This enabled the performance of a four-week measurement with two identical corrosion probes exposed on either side of the boiler. One probe exposed when AS was injected and the other one as Ref. Additionally, a ten-week corrosion measurement was carried out with injection of AS in both cyclones. The conditions were similar to those during a permanent installation of the ChlorOut concept. The amount of AS injected was controlled towards a fixed level of gaseous KCl by means of IACM. The corrosion probes were temperature controlled gradient probes with 18 different test rings as shown in Fig. 3.5. The temperature profile ranged from 400 to 555°C. Further information concerning the experimental and analytical procedure concerning deposit growth and metal loss by corrosion during the long-term measurements can be found in [40].

### 3.4 Modelling

In Paper V, the effect of volatile combustibles on the sulphation of gaseous KCl was modelled based on a detailed reaction mechanism. The reaction mechanisms originating from the Glarborg-Marshall mechanism [50] for formation of gaseous alkali sulphates were used in a chemical kinetic model (Chemkin). The mechanism consisted of subsets for H<sub>2</sub>/O<sub>2</sub> (O/H radical pool), alkali, sulphur and chlorine. They were updated by Hindiyarti et al. [49] concerning mainly SO<sub>2</sub> oxidation chemistry and K/Cl/S interactions [54, 61, 62]. The modelling was based on results presented in Paper IV.

Modelling based on experimental results has previously been performed at the Chalmers boiler focusing on the chemistry behind selective non-catalytic reduction (SNCR) of NO, and reduction of nitrous oxide (N<sub>2</sub>O) [75, 76]. The SNCR chemistry in Leckner et al. [75] was modelled treating the entrance of the cyclone, the cyclone itself and the exit duct as a plug flow reactor (PFR). The reduction of N<sub>2</sub>O in Gustavsson et al. [76] was modelled treating the gas movements in the cyclone as a perfectly stirred reactor (PSR). Here, a mean residence time ( $\tau$ ) of 0.5 seconds was calculated from the volume of the cyclone (8m<sup>3</sup>) at 900°C.

Fig. 3.6 shows the upper part of the combustion chamber and the cyclone with the three positions used for injection of ammonium sulphate. These were in the upper part of the combustion chamber (A in Fig. 3.6), in the cyclone inlet (B) and in the cyclone (C). Indata based on gas concentrations measured at these positions was selected. The reactor

model was a perfectly stirred reactor (PSR), which should represent the mixing conditions of the cyclone [76]. The influence of volatile combustibles on  $\text{SO}_3$  reduction was investigated by using different combinations of CO, methane, ethene and hydrogen. Ammonium sulphate was replaced by  $\text{SO}_3$  in the model.

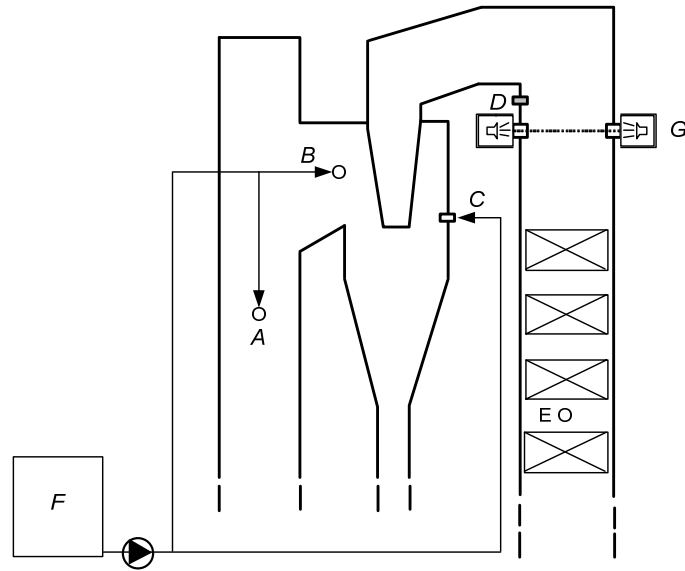


**Fig. 3.6.** A = upper part of the combustion chamber, B = the cyclone inlet, C = in the cyclone. D = before the convective pass, E = in the convective pass, F = Container with AS, G = IACM. A-C injection points for AS. D, E and G measurement positions.



## 4 KCl and flue gas chemistry

### 4.1 Transients, on-line fuel quality control

The molar ratio  $Cl/(K+Na)$  is often less than 1.0 during combustion of biofuels. Consequently, there is a lack of chlorine to form KCl which is demonstrated in Fig 4.1. Here, KCl is less than 5 ppm during combustion of pure wood pellets. The introduction of straw pellets as additional fuel started at  $t=60$  minutes and as a result, KCl rose immediately to 20 ppm. Co-combustion with PVC started at  $t=90$  minutes with KCl increasing further to approximately 70 ppm. KCl increased despite no additional alkali being supplied, verifying the lack of chlorine to form KCl during co-combustion of only wood and straw pellets.

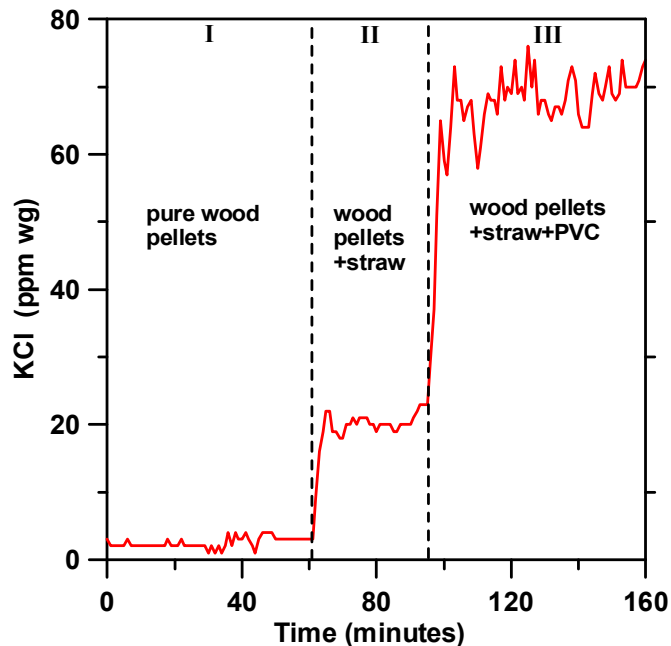


**Fig. 4.1.** Influence of K and Cl supply for formation of KCl. I. Pure wood pellets only, II. Supply of straw and wood pellets, III. Additional supply of PVC.

Fig. 4.2 shows transient tests from starting procedures during co-combustion with peat and injection of ammonium sulphate. KCl was measured by means of IACM before the convection pass and  $SO_2$  and HCl were measured by FTIR before the stack (23) in Fig. 3.1. The transient test during co-combustion with peat is shown in Fig. 4.2a. The gas phase concentration of KCl was less than 5 ppm during combustion of pure wood pellets (I). Straw pellets were introduced as additional fuel at  $t = 20$  minutes and as a result the concentration of KCl rose to 40 ppm (II). Co-combustion with peat started at  $t = 45$  minutes and the level of gaseous KCl decreased to 30 ppm. It was also observed that the

concentrations of SO<sub>2</sub> and HCl increased to more than 100 ppm and 70 ppm respectively. The increase in HCl was greater than the decrease in gaseous KCl (III), suggesting the occurrence of sulphation of KCl and/or reactions capturing K during the release of HCl. These reactions could occur in the gas phase as well as on particles in the convection section of the boiler. Such particles could either be present in the flue gas or deposited on colder surfaces such as boiler tubes in the convection pass.

The transient test for ammonium sulphate is shown in Fig. 4.2b. The level of gaseous KCl was 40 ppm during combustion of wood pellets with 25% straw pellets. AS was injected (S/Cl=1.0) at t = 35 minutes and KCl, SO<sub>2</sub>, HCl responded directly (II). The flow of AS was increased to an S/Cl of 1.5 at t = 75 minutes and once more an immediate change was observed in the gas phase concentrations of KCl, SO<sub>2</sub> and HCl. Sulphation of KCl in the gas phase according to (R4) is a fast reaction and the immediate decrease of KCl during injection of AS proved that a gas phase reaction had occurred. A comparison of the transient tests for peat and AS reveals significant differences. Although the concentration of SO<sub>2</sub> is higher during co-combustion with peat, the reduction of KCl is less efficient. Thus the sulphur in ammonium sulphate (i.e. SO<sub>3</sub>) is more efficient for the reduction of gaseous KCl than the sulphur in peat (i.e. SO<sub>2</sub>). Alkali capture reactions, with KCl and the ash-forming elements (i.e. Al, Fe, Ca and Si), taking place before (20) would also decrease KCl and increase HCl during co-combustion with peat.

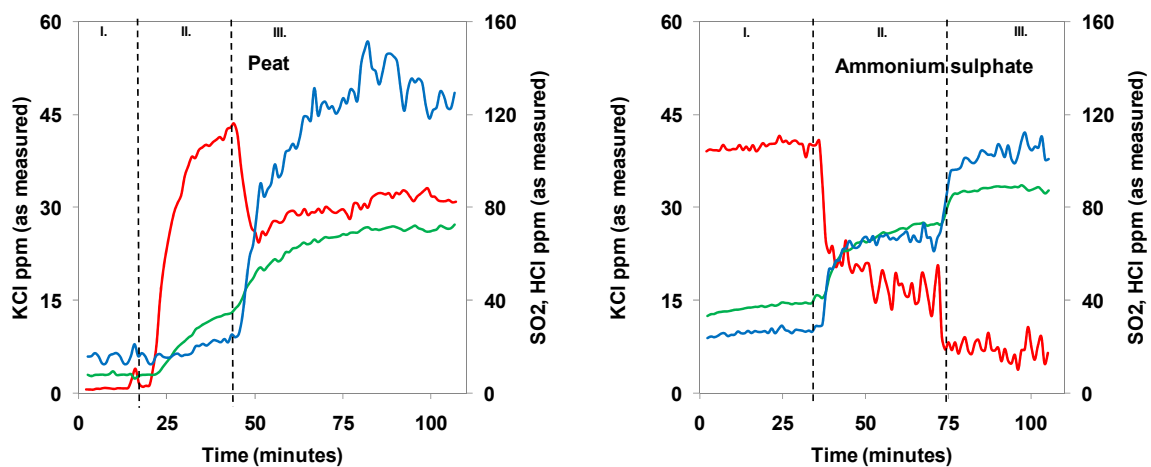
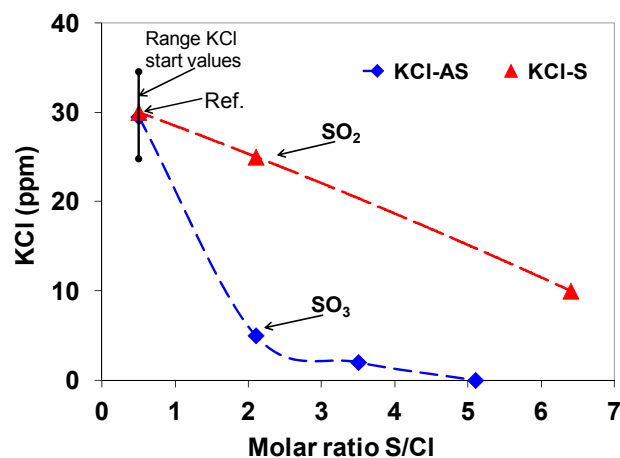


Fig. 4.2. KCl, SO<sub>2</sub> and HCl in transient tests during co-combustion of peat (a) and injection of ammonium sulphate (AS) (b). — KCl IACM, — SO<sub>2</sub> FTIR, — HCl FTIR. Peat (a) I. Wood pellets only, II. Supply of straw pellets, III. Peat replaced the wood pellets. Ammonium sulphate (b) I. Wood pellets and straw pellets, II. Injection of 5 l/h AS (S/Cl=1.0), III. Injection of 10 l/h AS (S/Cl=1.5).

## 4.2 Importance of SO<sub>2</sub>/SO<sub>3</sub> on sulphation of gaseous KCl

Paper II compares the performance of two sulphur/sulphate-containing additives: elemental sulphur (S) and ammonium sulphate (AS). These additives have previously only been compared very briefly [39, 41]. A key issue was to achieve a greater understanding of the importance of different forms of gaseous sulphur (SO<sub>2</sub>, SO<sub>3</sub>) for the

sulphation of gaseous KCl. The concentration of gaseous KCl versus the molar ratio S/Cl is shown in Fig. 4.3 for test cases Ref, AS and S. The average concentration of KCl was approximately 30 ppm during Ref and the start values of KCl before addition of the additives ranged between 26 and 36 ppm as indicated in Fig. 4.3. KCl was reduced from the average concentration of 30 ppm to 5 ppm at AS1 (S/Cl = 2.1) and to 2 ppm at AS2 (S/Cl = 3.5), but only to 10 ppm at test case S3 (S/Cl = 6.4). Sulphation of gaseous KCl was more efficient with AS even when the S/Cl molar ratio was less than half compared to sulphur. These results prove that the presence of SO<sub>3</sub> is of greater importance than that of SO<sub>2</sub> for gaseous sulphation of KCl.



**Fig. 4.3.** KCl versus the molar ratio S/Cl for ammonium sulphate (SO<sub>3</sub>) and elemental sulphur (SO<sub>2</sub>). AS was added at (18) in Fig. 3.1 and S at (14).

### 4.3 Effect of oxygen and combustibles on sulphation of KCl

Two experimental procedures were applied in Paper IV in order to study the effect of oxygen and combustibles on the sulphation of gaseous KCl. The influence of oxygen was studied by injection of AS into the cyclone at three air excess ratios ( $\lambda = 1.1, 1.2$  and  $1.4$ ). It was in the transient test investigated whether the presence of combustibles has an impact on the sulphation efficiency of gaseous KCl. Increasing amounts of ammonium sulphate were injected in a sequence during the transient tests. AS was injected in three positions at excess air ratios  $\lambda = 1.1, 1.2$  and  $1.4$ . These positions were in the upper part of the combustion chamber (17 in Fig. 3.1), in the inlet of the cyclone (18) and in the cyclone (19). Injection in an earlier position such as (17) results in longer residence times for sulphation of gaseous KCl. However, the sulphation in an earlier position could prove to be less efficient due to the composition of the flue gas.

The purpose of the transient test was to study how the gas composition at the injection point of AS influenced the sulphation of gaseous KCl. Since no additional secondary air is added after (5) in Fig. 3.1, the oxygen content was similar for the measurements during a specific air excess ratio. The presence of combustibles such as CO, hydrogen (H<sub>2</sub>), methane (CH<sub>4</sub>) and ethene (C<sub>2</sub>H<sub>4</sub>) could interact with the sulphation of KCl.

Fig. 4.4 show the concentration of CO and HC<sub>tot</sub> (volatile hydrocarbons) respectively at the three excess air ratios at six measurement locations. The air excess ratio had a major impact on CO and the highest concentration (> 6000 ppm) was found in the upper part of the combustion chamber at  $\lambda = 1.1$ . The concentration of CO was above 1000 ppm during all air excess ratios in the upper part of the combustion chamber. CO was much lower in the inlet of the cyclone despite remaining above 1000 ppm for  $\lambda = 1.1$ , and 1.2. The level of CO in the cyclone ranged from 50 ppm at  $\lambda = 1.4$  to approximately 800 ppm at the lowest air excess ratio. The level of HC<sub>tot</sub>, Fig. 4.4b, shows a similar pattern with the highest concentrations in the upper part of the combustion chamber, although only 50 ppm or less remained in the cyclone.

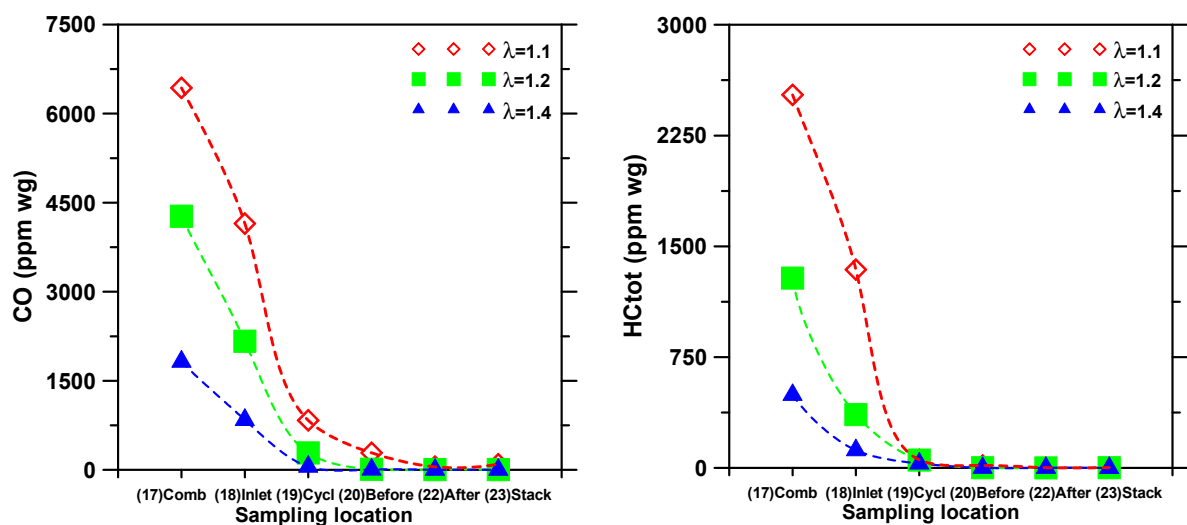


**Fig. 4.4.** CO (a) and HC<sub>tot</sub> (b) versus sampling location at excess air ratios  $\lambda = 1.1, 1.2$  and 1.4. The sampling locations were in the upper part of the combustion chamber (17 in Fig. 3.1), inlet of the cyclone (18), in the cyclone (19), before the convection pass (20), after the convection pass (22), and before the stack (23).

The concentration of gaseous KCl in Fig. 4.5 was approximately 45 - 50 ppm during each of the reference cases (Ref) without any injection at  $\lambda = 1.1$ . KCl was reduced to approximately 30 ppm during test case AS1 ( $S/Cl = 1.2$ ) when injecting AS to the cyclone. A significantly greater amount of AS ( $S/Cl = 2.5$ ) was required to obtain a similar reduction in the cyclone inlet. KCl was only lowered to approximately 35 ppm during the highest flow of AS (AS6,  $S/Cl = 4.6$ ) when injecting in the upper part of the combustion chamber. These tests revealed that the position had a great impact on the sulphation efficiency for gaseous KCl. The injection point in the upper part of the combustion chamber is characterised by a higher concentration of both CO and HC<sub>tot</sub> as can be seen in Fig. 4.4. The concentration of SO<sub>3</sub> was thus limited by the presence of combustibles (i.e. CO and/or volatile hydrocarbons). Consequently, SO<sub>3</sub> was partly consumed by other reactions than R4 which lowered the sulphation efficiency. The sulphation of KCl was also less efficient in the upper part of the combustion chamber at  $\lambda = 1.2$  (Fig. 5, Paper IV)



Sulphation of gaseous KCl (R4) results in an increase of HCl which should resemble the reduction of KCl in ppm. HCl was approximately 20 – 30 ppm during Ref in Fig. 4.5 and the greatest increase of HCl took place when injecting AS to the cyclone. Here, HCl increased by 32 ppm and the corresponding decrease of KCl was 28 ppm at a molar ratio S/Cl of 2.5. A slight difference between the increase of HCl and the decrease of KCl suggests gaseous sulphation of KCl rather than a heterogeneous reaction. The increase and decrease typically differed 2 – 5 ppm during the transient tests at  $\lambda = 1.1$ . The difference was similar or somewhat greater than it was at  $\lambda = 1.2$  (Fig. 6, Paper IV).

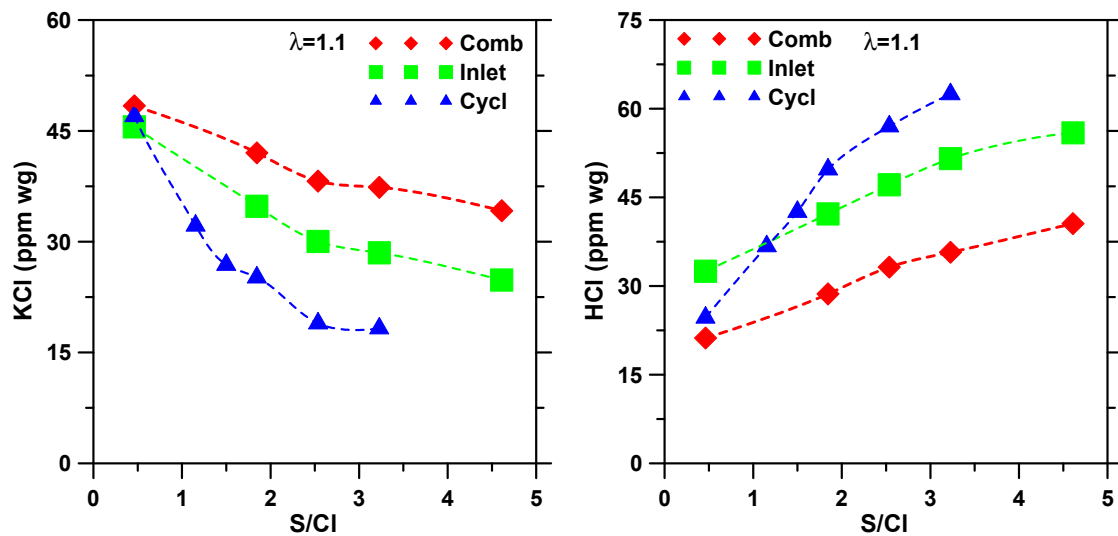
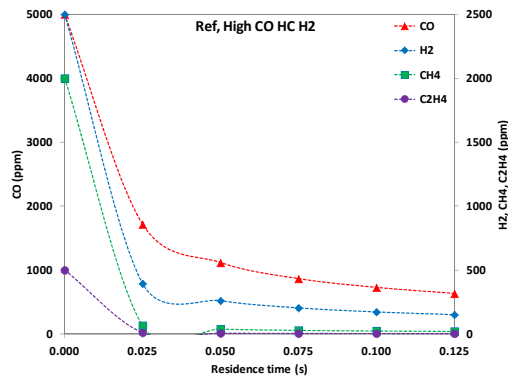


Fig. 4.5. Concentration of KCl (a) and HCl (b) versus molar ratio S/Cl during the transient test at excess air ratio  $\lambda = 1.1$ . AS was injected in the upper part of the combustion chamber (Comb, 17 in Fig. 3.1), in the cyclone inlet (Inlet, 18), and in the cyclone (Cycl, 19).

#### 4.4 Modelling the effect of volatile combustibles

The results from the modelling in Paper V were presented in three parts. First the reactor conditions (residence time) were evaluated to describe the sensitivity of the results. Secondly the influence of volatile combustibles on the sulphation of KCl is discussed and qualitatively compared to the experimental observations in Paper IV. Finally the reaction system was evaluated to decide on crucial reactions for the sulphation of KCl.

The sensitivity analysis revealed that a residence time of only 0.05 second was sufficient for all  $\text{SO}_3$  to react at both high and low level of combustibles. Fig. 4.6 shows the concentration of volatile combustibles and radicals generated in the high combustible case at a molar ratio S/Cl = 0.5. In this case, the volatile combustibles are consumed forming chain carrying radicals. There was no radical formation when the concentration of volatile combustibles was low. A residence time of 0.5 seconds and a temperature of 875°C were chosen as base case in the investigation.



**Fig. 4.6a.** CO, CH<sub>4</sub>, C<sub>2</sub>H<sub>4</sub> and H<sub>2</sub> versus residence time ( $\tau$ ) at high inlet concentrations of CO, HC<sub>tot</sub> and H<sub>2</sub>.

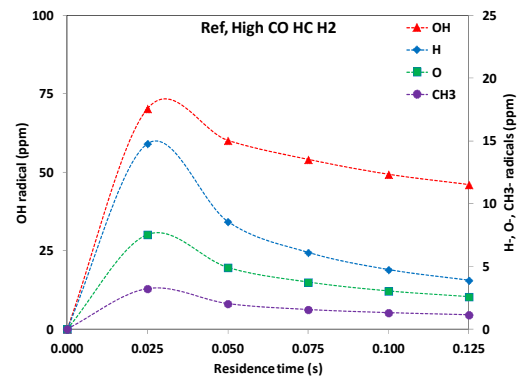


**Fig. 4.6b.** OH, H, O and CH<sub>3</sub> radicals versus residence time ( $\tau$ ) at high inlet concentrations of CO, HC<sub>tot</sub> and H<sub>2</sub>.

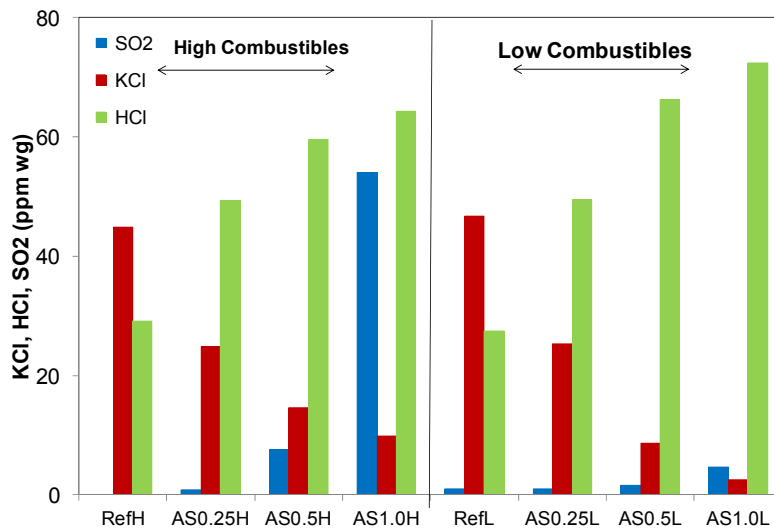


**Fig. 4.7.** Influence for KCl, HCl and SO<sub>2</sub> of the level (low and high) of volatile combustible present at injection of AS at different levels. The molar ratios S/Cl were 0, 0.25, 0.5, 1.0.

The influence of volatile combustibles was investigated by using different combinations of CO, methane, ethene and hydrogen. The outlet O<sub>2</sub> concentration was kept constant (around 1%). Fig. 4.7 shows the modelled influence for KCl, HCl and SO<sub>2</sub> of the level (low and high) of volatile combustible present at injection of AS at different levels (S/Cl molar ratios). It is observed that the sulphation of KCl was less efficient and SO<sub>2</sub> formation from SO<sub>3</sub> occurred in the presence of high levels of combustibles.

In the investigated system, SO<sub>3</sub> is added with the purpose of oxidising KCl to K<sub>2</sub>SO<sub>4</sub>. The major reactions paths for SO<sub>3</sub> are presented in Fig. 4.8. SO<sub>3</sub> may either react with KCl through the desired path to K<sub>2</sub>SO<sub>4</sub> or with H and HO<sub>2</sub> radicals forming SO<sub>2</sub>. However, as proposed in [49], there could be a sulphation pathway that bypasses SO<sub>3</sub> through the formation of KSO<sub>4</sub> (dotted line in Fig. 4.8). In the present investigation, this pathway

favours sulphation of KCl in the presence of combustibles to almost the same levels as the  $\text{SO}_3$  pathway. The experimental result, however, indicates a higher influence of combustibles. This could be caused by either model assumptions (e.g. residence time, mixing conditions, species concentrations) or an overestimation of the  $\text{SO}_2$  sulphation capacity.

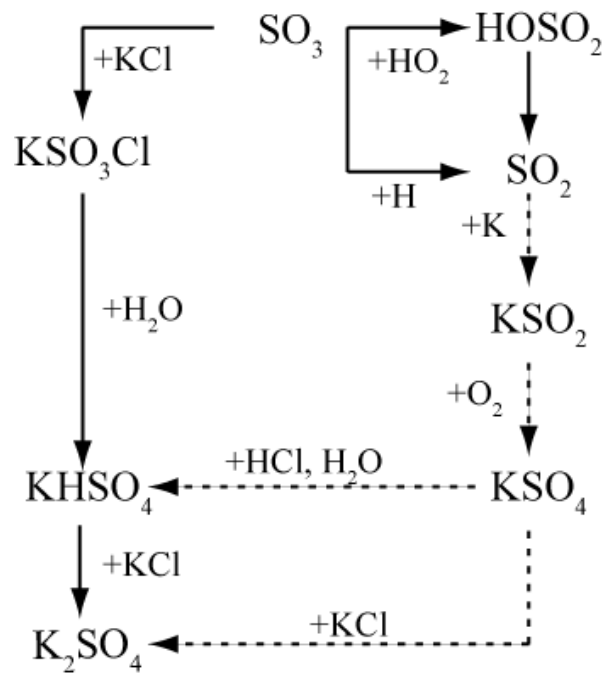


**Fig 4.8.** Major reaction pathways of  $\text{SO}_3$  in the investigated system. Solid lines indicate paths of importance for the sulphation of KCl by  $\text{SO}_3$  and dashed lines indicate paths important for sulphation of KCl by  $\text{SO}_2$ .

#### 4.5 Summarised results concerning sulphation of gaseous KCl

The experimental results from IACM revealed that the sulphation of gaseous KCl was less efficient when ammonium sulphate was injected in the upper part of the combustion chamber and during lower air excess ratios. An earlier position, such as the upper part of the combustion chamber, gives a less efficient sulphation although the residence time is longer in comparison with the other positions during the same air excess ratio. The burn-out of combustibles is, however, more complete in the downstream positions which leads to less interactions for  $\text{SO}_3$  with the O/H radical pool [54]. It is observed in Fig. 4.5 that the position seems to have a greater impact on the sulphation efficiency of KCl than the air excess ratio.

Fig. 4.9 shows measured KCl versus molar ratio S/Cl during the best and worst combination of position and air excess ratio. It is also shown that a similar reduction of KCl can be achieved at the three positions by a combination of position and air excess ratio. The reduction of gaseous KCl was similar in the upper part of the combustion chamber at  $\lambda = 1.4$ , in the inlet of the cyclone at  $\lambda = 1.2$  and in the cyclone at  $\lambda = 1.1$ . The

chamber at  $\lambda = 1.4$ , in the inlet of the cyclone at  $\lambda = 1.2$  and in the cyclone at  $\lambda = 1.1$ . The most efficient sulphation was achieved during injection of AS in the cyclone at  $\lambda = 1.4$  whereas the poorest sulphation was in the upper part of the combustion chamber at  $\lambda = 1.1$ . The injection point in the cyclone is characterised by sufficiently high concentration of  $O_2$  and low concentration of volatile combustibles. This minimises the formation of  $SO_2$  from  $SO_3$  (R3) and the consumption of  $SO_3$  from reactions with H radicals (R8). The injection point in the upper part of the combustion chamber is characterised by both rather low concentration of  $O_2$  and the presence of volatile combustibles such as CO, hydrogen, methane and ethene. These conditions favoured the formation of  $SO_2$  from  $SO_3$  (R3) and the consumption of  $SO_3$  from reactions with H radicals (R8). These results were compared with those in Fig. 5.3 showing the reduction of KCl when using AS (i.e.  $SO_3$ ) and sulphur (i.e.  $SO_2$ ). The performance of AS during injection in the upper part of the combustion chamber at  $\lambda = 1.1$  resembled the sulphation efficiency for KCl when adding sulphur rather than AS in an appropriate position. The formation of  $SO_2$  according to R8 from  $SO_3$  and H radicals is a fast reaction. The oxidation of  $SO_2$  back to  $SO_3$  (R3) is the rate-limiting step when adding sulphur. The appropriate position and conditions for injection of AS in a full-scale boiler can be identified by measuring KCl with IACM.

Fig. 4.10 shows the modelled concentration of KCl versus molar ratio S/Cl. The sulphation of KCl was also less efficient in the presence of high levels of combustibles according to the model. The high and low level of the simulations were set to correspond to the measurement cases with the blue line (Cycl  $\lambda=1.4$ ) and red red line (Comb  $\lambda=1.1$ ) in Fig. 4.9. The modelled influence from the presence of combustibles corresponded to the measured influence, although, the influence of combustibles were underestimated.

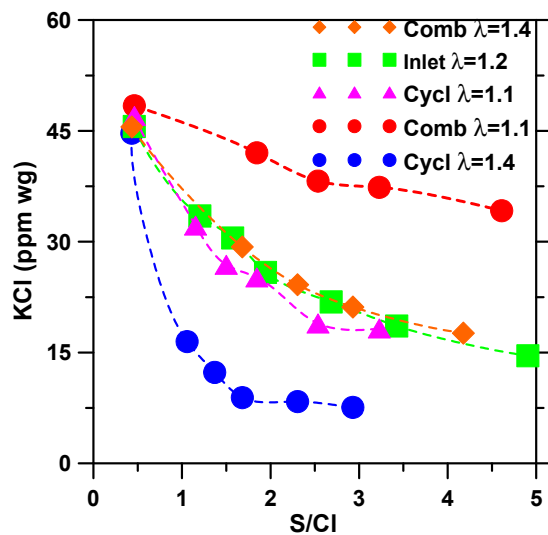


**Fig. 4.9.** Measured concentration of KCl versus molar ratio S/Cl during the best (Cycl  $\lambda=1.4$ ) and worst (Comb  $\lambda=1.1$ ) combination of position and air excess ratio for reduction of gaseous KCl. The combinations with similar reduction of KCl (Comb  $\lambda=1.4$ , Inlet  $\lambda=1.2$  and Cycl  $\lambda=1.1$ ).

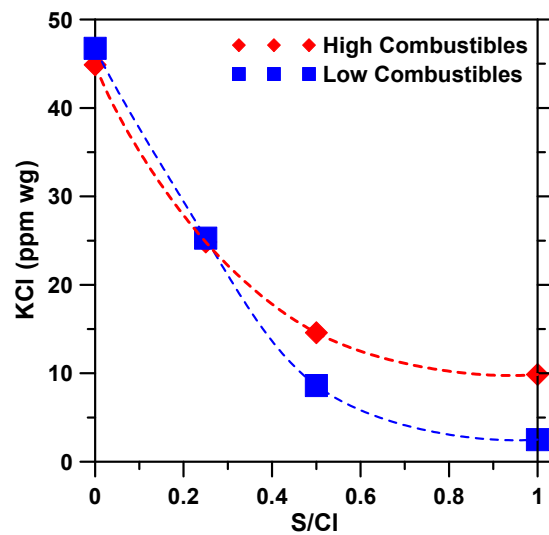


**Fig. 4.10.** Modelled concentration of KCl versus molar ratio S/Cl in the presence of high and low levels of combustibles

## 5 Strategies to reduce KCl and chlorine in deposits

This chapter describes experimental results, focusing on the strategies applied in Papers II, III and IV to reduce gaseous KCl and chlorine in deposits in order to prevent deposit formation and superheater corrosion. Further information about the experimental and analytical procedures as well as additional results can be found in the corresponding Papers. Certain results concerning sulphation of gaseous KCl have already been presented in chapter 5 and are consequently treated in less detail here.

### 5.1 Sulphur/sulphate-based additives

#### 5.1.1 Elemental sulphur and ammonium sulphate

The performance of elemental sulphur and ammonium sulphate for the sulphation of gaseous KCl was compared in section 4.2. The sulphation of KCl was more efficient with AS even when the S/Cl molar ratio was less than half compared to sulphur. These results proved that the presence of  $\text{SO}_3$  is of greater importance than that of  $\text{SO}_2$  for gaseous sulphation of KCl. Deposits collected during the reference case (Ref), consisted mainly of K and Cl. These deposits contained less Cl and more S when sulphur was added, and no chlorine was detected at all when AS was injected. The mole-% of K, Cl and S is shown in Fig. 5.1, and KCl, present in Ref, was already fully sulphated at AS2 (S/Cl=3.5) when using AS and only partly sulphated using sulphur in S3 (S/Cl=6.4). The sulphation was more efficient in AS2 although the molar ratio S/Cl was significantly lower than in S3.

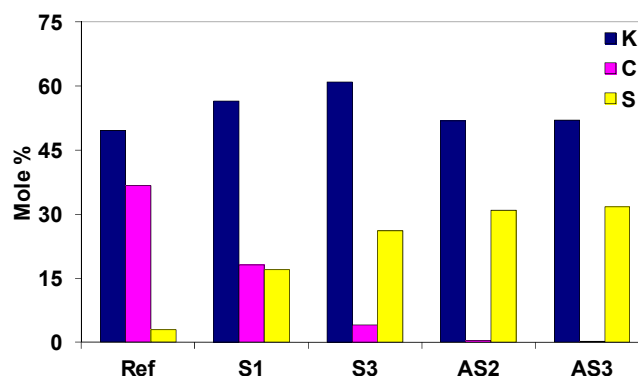


**Fig. 5.1.** Mole % of K, Cl and S in the deposits. Test cases Ref (S/Cl=0.5), S1 (S/Cl=2.1), S3 (S/Cl=6.4), AS2 (S/Cl=3.5) and AS3 (S/Cl=5.1).

Fig. 5.2 shows the SEM image (to the left) and the corresponding EDX maps of K, Cl and S from selected deposit steel rings exposed in the test cases. The lighter parts represent the presence of a specific element in the particles. The deposit mainly consisted of K and Cl during Ref and the distribution of these elements correlated well in Fig 5.2a. Fig. 5.2b is from test case S1 and it is noticed that the deposits still contained mainly K

and Cl. Fig. 5.2c shows SEM analysis from case S3 and here the deposits consisted mainly of K and S and their distribution correlated. EDX maps from case AS1 are shown in Fig. 5.2d and the deposit consisted of K and S. The deposit was already fully sulphated at the lowest dosage of ammonium sulphate (AS1), whereas at the highest dosage of sulphur (S3) a similar or somewhat lower degree of sulphation was achieved. Thus elemental sulphur was not as effective as ammonium sulphate in preventing chlorine in the deposits on heat transfer surfaces in the convection pass of the boiler.

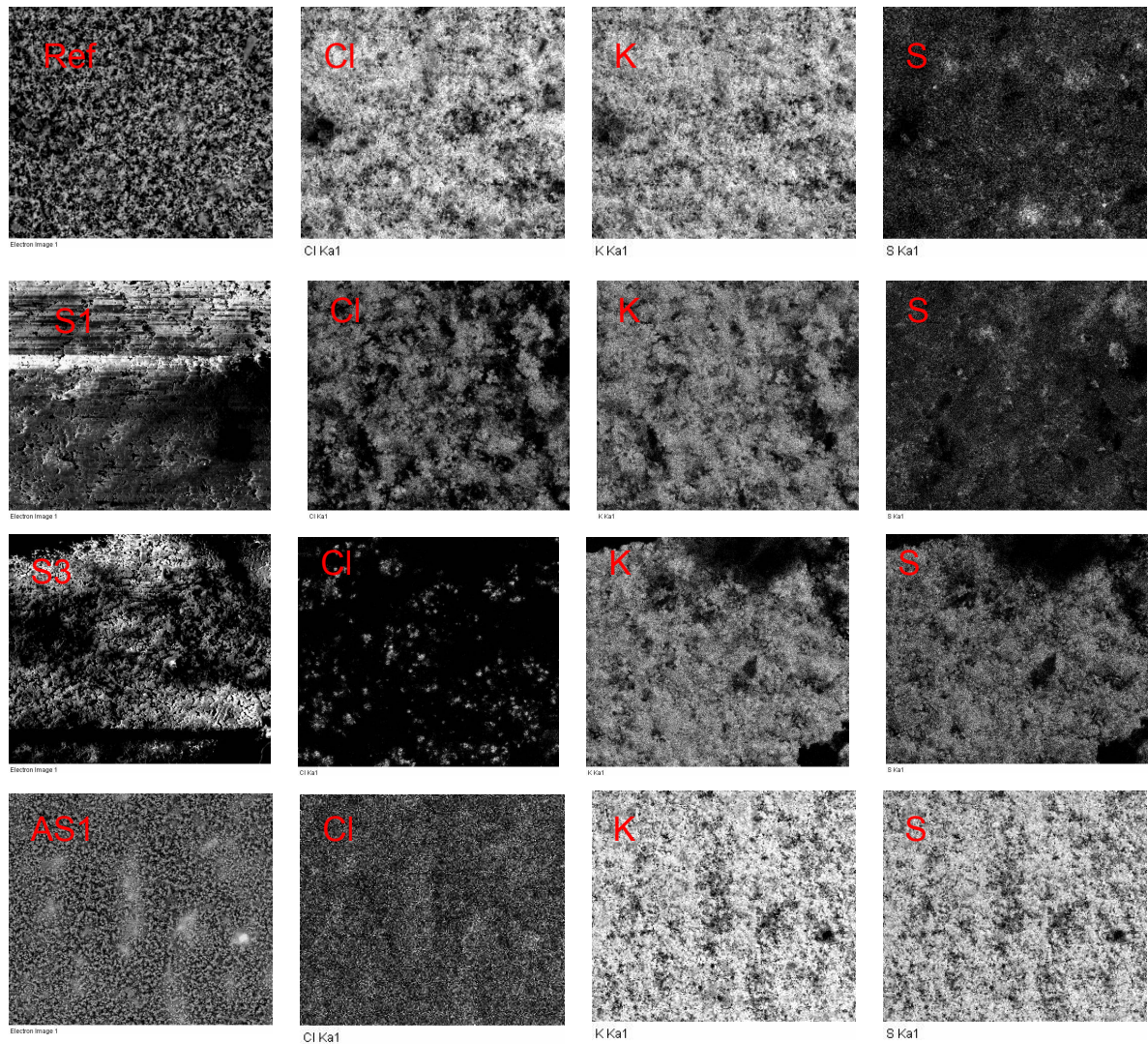


**Fig. 5.2.** SEM image to the left and EDX maps according to element labels of K, Cl and S from deposits collected at different test cases. a) Ref (S/Cl = 0.5), b) S1 (S/Cl = 2.1), c) S3 (S/Cl = 6.4), d) AS1 (S/Cl = 2.1).

### 5.1.2 Influence of O<sub>2</sub> on sulphation of KCl and chlorine in deposits

The presence of combustibles could interact with the effect of oxygen on the sulphation of gaseous KCl making the evaluation less obvious. The concentration of combustibles was lower in the cyclone in comparison with the upper part of the combustion chamber and in the cyclone inlet. Consequently, the effect of oxygen on sulphation was studied by injecting AS into the cyclone (19 in Fig. 3.1). The air excess ratios selected were  $\lambda = 1.1$ , 1.2 and 1.4, and the operating parameters for each ratio are presented in Paper IV. The test cases Ref, ASL and ASH corresponded to a molar ratio S/Cl of 0.5, 1.4 and 2.8 respectively at  $\lambda = 1.2$ .

Fig. 5.3 shows the concentration of gaseous KCl versus the molar ratio S/Cl, KCl being approximately 50 ppm during the reference cases at the different air excess ratios. KCl was reduced to 13 ppm at a  $\lambda$  of 1.4 and to 20 ppm at a  $\lambda$  of 1.2 during test case ASL. The reduction of KCl was less efficient during the lowest air excess ratio. Twice the amount of AS (ASH) was required for  $\lambda = 1.1$  to obtain a reduction similar to ASL at  $\lambda = 1.2$ . This suggests the concentration of O<sub>2</sub> had an impact on the sulphation efficiency when injecting AS in the cyclone. The equilibrium of R3 is moved towards SO<sub>2</sub> at lower  $\lambda$  and the formation of SO<sub>2</sub> from SO<sub>3</sub> could possibly explain the poorer sulphation during the lower air excess ratios. The presence of combustibles could also have had a considerable influence on the sulphation of KCl although the cyclone was selected to minimise its contribution. Fig. 4.4a shows that the concentration of CO in the cyclone ranged from 50 ppm at  $\lambda = 1.4$  to approximately 800 ppm at the lowest air excess ratio. The presence of volatile hydrocarbons in the cyclone is shown in Fig. 4.4b and 50 ppm or less of HC<sub>tot</sub> remained. The low levels of volatile hydrocarbons in the cyclone suggest that the results obtained were to a large extent an effect of the O<sub>2</sub> concentration.

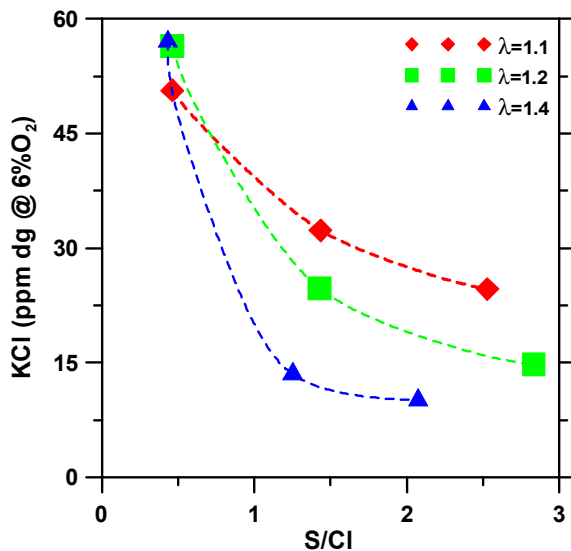


Fig. 5.3. KCl versus molar ratio S/Cl during injection of AS in the cyclone at the three air excess air ratios (-  $\lambda = 1.1$ , --  $\lambda = 1.2$ , --  $\lambda = 1.4$ ).

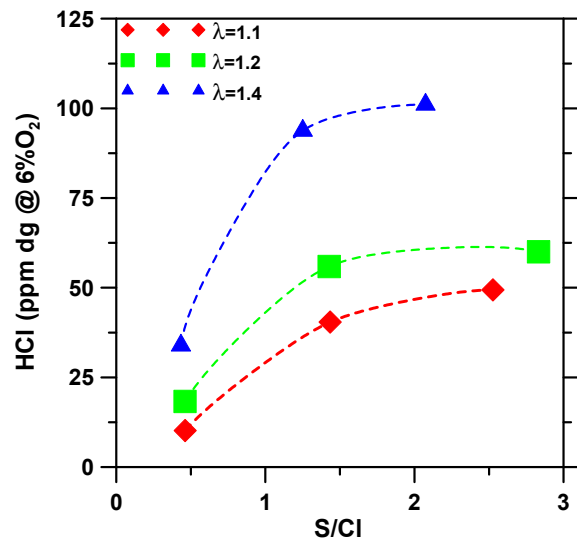
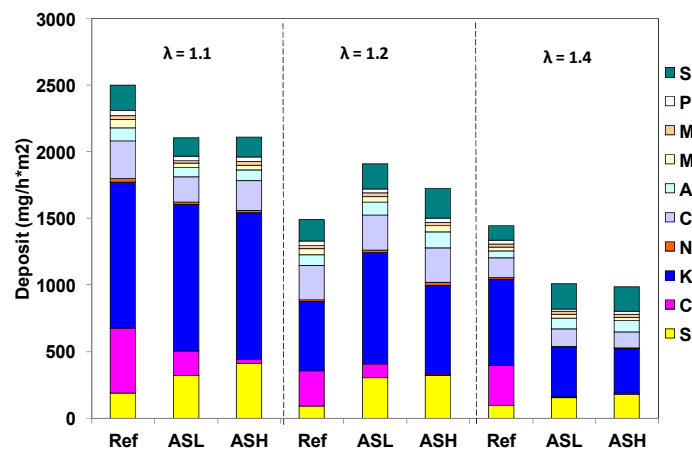


Fig. 5.4. HCl versus molar ratio S/Cl during injection of AS in the cyclone at the three air excess air ratios (-  $\lambda = 1.1$ , --  $\lambda = 1.2$ , --  $\lambda = 1.4$ ).

Fig. 5.4 shows HCl measured after the convection pass (22 in Fig. 3.1). HCl is expected to increase during gaseous sulphation of KCl (R4), and a higher concentration was noticed during all test cases compared to the reference cases. The increase of HCl should, according to R4, correspond to the decrease in KCl during gaseous sulphation of KCl. A greater increase of HCl than the decrease of gaseous KCl can be explained by gaseous sulphation between the measurement location for KCl (19) and that for HCl (22). It can also be explained by secondary sulphation of KCl condensed on particles or colder surfaces such as boiler tubes. Further results concerning other gas components are shown in Paper IV (Table 5).



**Fig. 5.5.** Composition of deposits given as elements during injection of ammonium sulphate in the cyclone for test cases Ref, ASL and ASH at excess air ratios  $\lambda = 1.1, 1.2$  and  $1.4$ .

Deposit measurements were also carried out and Fig. 5.5 shows the composition in deposits from the whole ring. The main elements were S, Cl, K, Ca and Si. Significantly more chlorine and less sulphur were found in the deposits in the reference cases when no AS was injected during all  $\lambda$ . In general, the deposit growth rate was greater during lower excess air ratios and injection of AS lowered the growth rate somewhat. The mole-% of Cl versus the molar ratio S/Cl during the Ref, ASL and ASH cases are shown in Fig. 5.6. The highest mole-% of Cl was found in the deposits during the reference cases. Significant amounts of Cl were also found for ASL at  $\lambda = 1.1$ . Nevertheless, only low amounts of chlorine remained during ASH at  $\lambda = 1.1$ . Chlorine was reduced although a significant concentration of KCl was measured by IACM suggesting a contribution from heterogeneous sulphation as well. No chlorine was detected in the deposits even at a molar ratio S/Cl of only 1.3 (ASL) during the highest  $\lambda$ . KCl present in the flue gas and in the deposit during Ref was already fully sulphated at ASL during  $\lambda = 1.4$  and only partly sulphated at ASL during  $\lambda = 1.1$ . The sulphation was even somewhat better during ASL ( $\lambda = 1.4$ ) than ASH during  $\lambda = 1.1$ . The more efficient sulphation was achieved although the molar ratio S/Cl was 2.5 at  $\lambda = 1.1$  and only 1.3 during  $\lambda = 1.4$ . The mole-% of S



increased in the deposits at increasing molar ratios S/Cl. However, it was not possible to identify any significant differences due to the air excess ratio.

The results in Figs. 5.3 and 5.6 reveal a clear correlation between the sulphation of gaseous KCl and reduced chlorine content in the deposits in most test cases. Thus on-line measurements of KCl by IACM can give an indication of the risk for increased chlorine content in the deposits during operation of full-scale boilers.

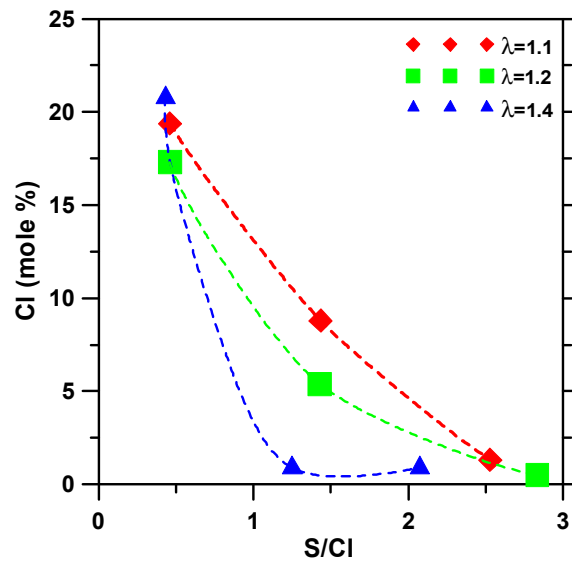


**Fig. 5.6.** Mole % of chlorine (Cl) in the deposits versus molar ratio S/Cl during injection of ammonium sulphate in the cyclone at three different excess air ratios ( $\lambda = 1.1, 1.2, 1.4$ ).

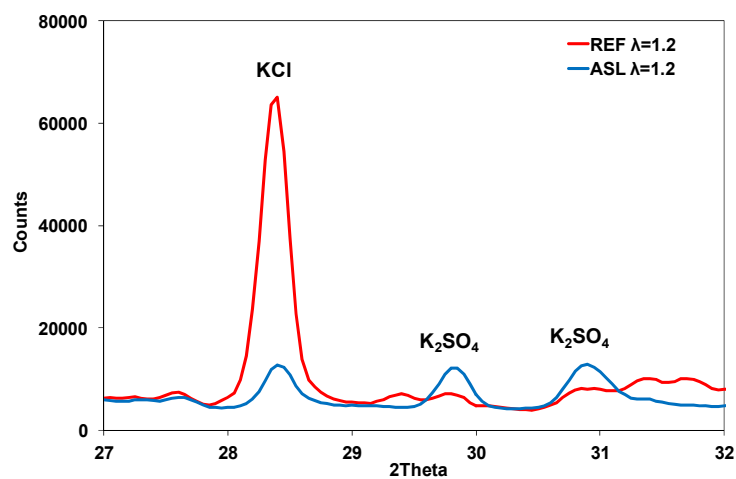


**Fig. 5.7.** XRD deposit analyses showing the largest KCl and  $K_2SO_4$  peaks during  $\lambda=1.2$  for Ref and ASL.

XRD-measurements were performed on the deposits [77]. The results showed that KCl and  $K_2SO_4$  are the main compounds in the deposit. Fig. 5.7 shows the diffraction patterns

for  $\lambda=1.2$  at  $27 < 2\Theta < 32$  illustrating the changes in intensity for the strongest KCl and  $K_2SO_4$  peaks. Injection of AS (ASL) decreased the intensity of the KCl peak.

## 5.2 Ammonium sulphate and co-combustion of peat

Demonstrated in Paper III were two strategies to decrease the risk of superheater corrosion by reducing the concentration of gaseous KCl in the flue gas and the content of chlorine in deposits. These strategies were co-combustion of biomass with peat and injection of ammonium sulphate both of which were also investigated in a large-scale CFB boiler in Paper I. The main scope was to gain improved understanding of how gaseous KCl and chlorine in deposits are reduced during co-combustion with peat.

Fig. 5.8 shows the concentration of KCl,  $SO_2$  and HCl for test cases Ref, Peat, RefCl and ASCl. The measurements of KCl, and  $SO_2$  were performed by means of IACM before the convection section. The level of KCl was 39 ppm during Ref and only a minor reduction of KCl to 24 ppm was observed during test case Peat. The concentration of HCl in the flue gas increased during Peat compared to Ref and during ASCl compared to RefCl. The increase of HCl after the convective pass (22 in Fig. 3.1) was significantly higher than the reduction of gaseous KCl during Peat. This strongly indicates that heterogeneous sulphation or alkali capture on ash particles followed by release of HCl had also taken place. The overall increase in HCl was somewhat below 50 ppm. Accurate measurements of gaseous HCl in a particle rich environment such as in (22) pose a considerable challenge. In view of this, the increase of HCl corresponds reasonably well with a possible maximum decrease of up to 40 ppm KCl during Peat. The addition of PVC increased KCl to 95 ppm (RefCl), whereas it dropped to 13 ppm during test case ASCl. The injection of AS significantly lowered the level of gaseous KCl in the flue gas. The decrease of KCl was approximately 80 ppm and the corresponding increase of HCl was similar to 80 ppm. Thus gaseous KCl was mainly sulphated according to R4 during ASCl and the contribution from heterogeneous sulphation was less important. Further results from IACM and gas analysis for all test cases are shown in Table 4 in Paper III.

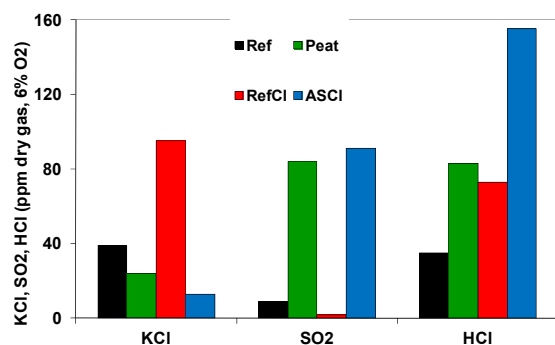


Fig. 5.8. Concentration of gaseous KCl,  $SO_2$  and HCl for test cases Ref, Peat, RefCl and ASCl.

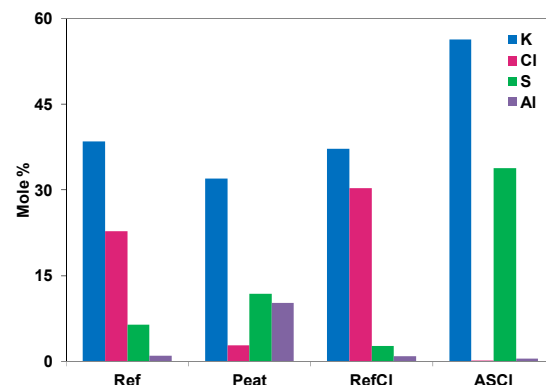
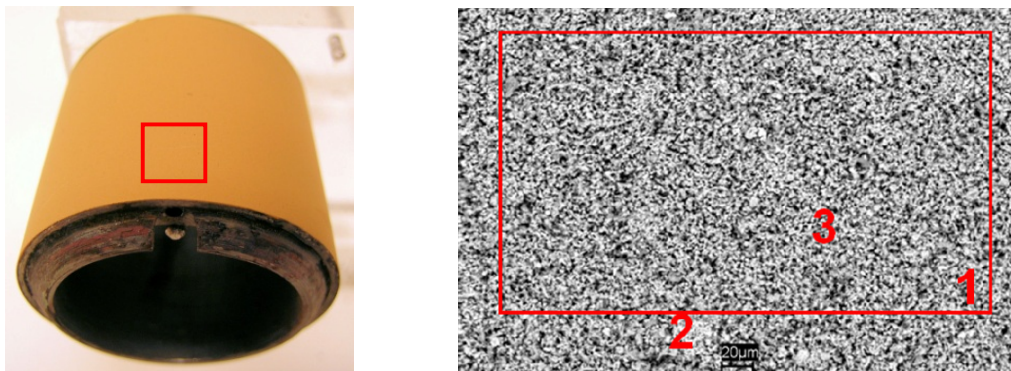


Fig. 5.9. Mole % of potassium (K), chlorine (Cl), sulphur (S) and aluminium (Al) in the deposits.

Deposits were collected on test rings after exposure at 500°C and the deposit growth rate was lower during test cases Peat and ASCl compared to the corresponding reference cases (Ref, RefCl). Wet chemical analysis was carried out on all the deposits collected. Fig. 5.9 shows K, Cl, S and Al for test cases Ref, Peat, RefCl and ASCl presented as mole %. During Ref the deposits consisted mainly of K and Cl. Much less Cl was found during Peat compared to Ref. The reduction of Cl was achieved although the content of sulphur remained low, suggesting that chlorine was reduced by capture of K during the release of Cl as HCl in parallel to sulphation. The highest chlorine content was present during RefCl. Nevertheless no chlorine was found in the deposits during ASCl when AS was injected at a molar ratio S/Cl of 1.0. The deposit consisted mainly of KCl during RefCl, which was fully sulphated during ASCl. The deposit contained significantly more aluminium during Peat compared to Ref.

The effect of injection of AS revealed that gaseous KCl was greatly reduced and the deposit was sulphated and contained no chlorine. Meanwhile, the effect of co-combustion of peat was less obvious although it is suggested that chlorine in the deposits was reduced by capture of K in parallel to sulphation. Consequently, the further evaluation focuses on test cases Peat and Ref.

Fig. 5.10 shows a photograph and an SEM image of the deposits collected on the ring made of 304L at 600°C for test case Peat. The colour of the deposits differed from the other test cases and probably due to the presence of ash components such as iron oxides originating from the peat. EDX quantification was performed as area and point analysis (Table 5.1). It was found that the deposit consisted of K and O together with the major ash forming elements S, Al, Fe, Ca and Si. This supports the hypothesis that an alkali capture reaction had occurred in parallel to sulphation of KCl. The photograph and SEM image of the deposits collected for test case Ref are shown in Paper III. The point analysis during Ref revealed that the deposit consisted mainly of K, Cl, S and O, suggesting the presence of KCl and K<sub>2</sub>SO<sub>4</sub>.



**Fig. 5.10.** SEM images of the 304L sample exposed for 4 hours at 600°C in test case Peat. The area marked in the left image is shown to the right.

Table 6.1. EDX quantifying of element composition in the points shown in Fig. 5.10.

Atomic %	O	K	Na	Mg	Ca	Al	P	S	Cl	Si	Fe
1 (sum)	62	15	1	1	3	3	1	7	0	4	3
2	44	17	0	1	5	3	1	8	0	2	19
3	64	11	1	1	3	4	1	6	0	4	4

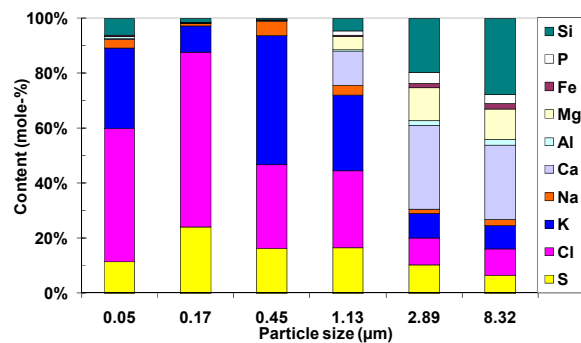


Fig. 5.11a. Chemical composition for different fly ash sizes collected by the impactor during test case Ref.

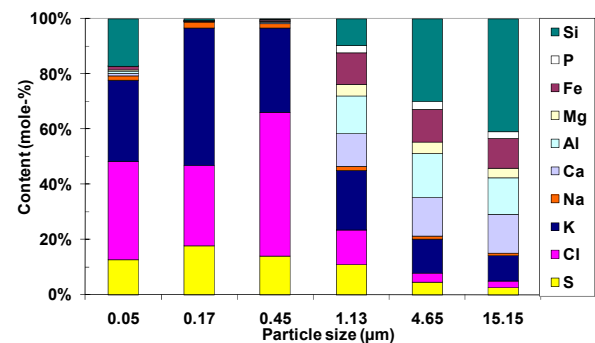


Fig. 5.11b. Chemical composition for different fly ash sizes collected by the impactor during test case Peat.

The chemical compositions of different particle sizes of fly ash particles were obtained from the LPI measurements and are shown in Fig. 5.11 for test cases Ref and Peat. Fine particles were composed of mainly potassium, chlorine and some sulphur during Ref. The fine particles during test case Peat also consisted of mainly potassium, chlorine and sulphur. Larger particles contained Si and Ca, but also increasing amounts of Al, and Fe during Peat. These elements (Al, Fe, Ca, Si) were also found in the deposits parallel to sulphur during Peat in Table 5.1, supporting the theory that alkali capture reactions had occurred in parallel to sulphation.

Wet chemistry and EDX quantification were applied in order to characterise the elements present in the deposits. A greater challenge is to determine the actual compounds in the deposits by XRD analysis. An attempt was made in Paper III to identify in which crystalline compounds alkali was captured. Although the ash particles on the deposit rings mainly formed non-crystalline phases, some indications are given. Arcanite ( $K_2SO_4$ ) was the major crystalline compound in the deposits during Peat. In addition, small amounts of potassium containing aluminium silicates ( $KAlSi_3O_8$ , ortholase) may be present during test case Peat. Sylvite (KCl) was a major crystalline compound together with arcanite during Ref. No crystalline iron oxides were identified in the deposits despite their colour (Fig. 5.10).

The initial corrosion was investigated by means of SEM-EDX analysis of the corrosion front. The initial corrosion analysis revealed that the strategies applied were also effective in lowering the initial corrosion attack. The initial chromium-rich oxide that normally

protects 304L from further oxidation showed signs of degradation already after 4 hours during Ref. The corrosion attack is suggested to have been initiated by the presence of KCl in the deposit formed. Laboratory experiments [32] have shown that the breakdown of 304L is triggered by a chromate formation reaction taking place in the presence of KCl. In contrast to the Ref exposure, the ASCl and Peat exposures showed no signs of initial corrosion of 304L. The oxide formed on the steel samples was instead chromium-rich and protective. Laboratory studies have shown that  $K_2SO_4$  does not accelerate the corrosion of 304L at  $600^\circ C$  (in contrast to KCl) [38]. The non-corrosive nature of  $K_2SO_4$  is explained by its relative thermodynamic stability. Hence, in contrast to KCl, the reaction of  $K_2SO_4$  with the protective oxide to form  $K_2CrO_4$  is not thermodynamically favoured. Thus, the protective oxide formed on 304L is not destroyed and the corrosion rate remains low.

### 5.3 Remarks concerning co-combustion with peat

The reduction of gaseous KCl was less efficient during co-combustion with peat, but chlorine content in the deposits was, nevertheless, greatly reduced. Additionally, the increase in HCl was greater than the reduction of gaseous KCl. This strongly indicates that heterogeneous sulphation or alkali capture on ash particles followed by release of HCl had also taken place.

Fig. 2.3 was used in Section 2.4 to present principal pathways for KCl during co-combustion of biomass with peat. K from KCl may be captured in the combustion chamber by means of reactions with ash minerals (2) and quartz sand particles (3). The ash minerals for alkali capture can originate from the additional fuel (i.e. peat). KCl may also be sulphated (4) in the combustion chamber by sulphur from peat. Gaseous KCl present in the flue gas after the combustion chamber may be sulphated by  $SO_2(g)/SO_3(g)$  (5). This sulphation can occur by sulphur species originating from peat. The concentration of gaseous KCl obtained by IACM is a measure of the importance of reactions taking place in the combustion chamber and in the flue gas.

KCl (s, l) condensed in deposits is disadvantageous, since deposits rich in chlorine may cause accelerated corrosion of especially low-alloyed superheater tubes. Increased corrosion rates were observed for the low alloyed steel 13CrMo44 when the deposits contained chlorine during the long-term measurement in Munksund. Furthermore, capture of K (6) by ash minerals during release of HCl may render the deposit less corrosive. Heterogeneous sulphation of KCl (s, l) by  $SO_2(g)/SO_3(g)$  (7) can also alter the deposit chemistry to a less corrosive state.

Reactions occurring in the combustion chamber and in the flue gas before measurement location (20) in Fig. 3.1 lowered KCl from 39 to 24 ppm during co-combustion with peat (see Fig 5.8). Consequently, reactions taking place in the flue gas after (20) or in the deposits according to (6) or (7) in Fig. 2.3 account for the low amount of chlorine found in the deposits. A possible explanation for this is sulphation of KCl or capture of K on reactive ash components (i.e. Al, Fe, Ca and/or Si) when using peat. The sulphur in peat can be oxidised to  $SO_2$  and  $SO_3$  during combustion and is believed to sulphate KCl in a similar way as described for elemental sulphur in Paper II.

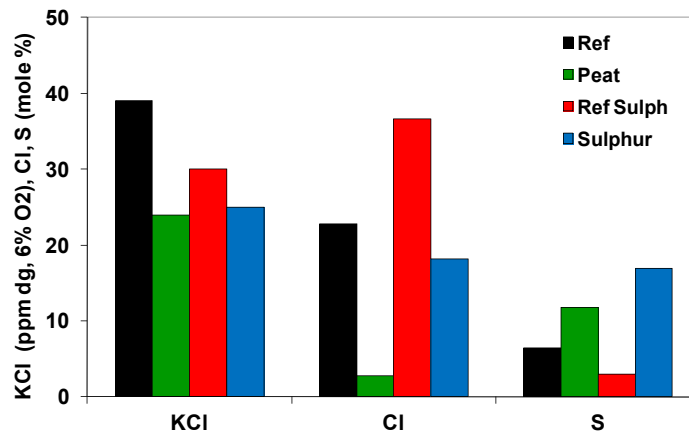


**Fig. 5.12.** Concentration of gaseous KCl, mole % Cl and S in the deposits during test cases Ref and Peat, compared to Ref Sulph and Sulphur from Paper II. The molar ratio S/Cl was 1.9 for Peat and 2.1 for Sulphur.

Sulphation of gaseous KCl was less important during the co-combustion with peat. Nevertheless, the chlorine content in the deposits was greatly reduced at a molar ratio S/Cl of 1.9. The test case S1 for sulphur in Paper II had molar ratio S/Cl of 2.1 which is similar to the ratio for test case Peat (S/Cl = 1.9). Fig 5.12 shows a comparison between S1 (here named Sulphur), Peat and their corresponding reference cases (Ref Sulph, Ref). Gaseous KCl was reduced by 15 ppm during Peat and only by 5 ppm during Sulphur. Even more obvious is the better performance for Peat in reducing Cl in the deposits. Almost no chlorine was present in the deposits during Peat although the sulphur content was lower than during Sulphur. Thus chlorine in the deposits was reduced by capture of K by ash minerals in parallel to sulphation during co-combustion with peat.

An attempt was made to identify which ash minerals in this particular peat type accounted for the capture of K. Deposit analysis revealed an increase in the ash-forming elements Al, Fe and Si. However, it was still not possible to identify the compounds in which alkali was captured by using XRD. The ash particles on the deposit rings mainly formed non-crystalline phases which can not be identified by XRD. As a result, the mechanism/chemistry by which the ash minerals in peat reduced the chlorine content in the deposits remained unidentified. The fraction of Al, Fe, Ca and Si in the deposits generally increased during Peat in comparison to test case Ref. These elements were also present in higher mole-% for Peat compared to Ref in the coarser fractions (stages > 1  $\mu\text{m}$ ) during the impactor measurements as shown in Fig 5.11. Ash particles containing Al, Fe Ca and Si in the flue gas could act as adsorption/condensation surfaces of gaseous KCl and/or is the elements in the peat ash reacting with KCl (s,l,g) (according to (6) in Fig 2.3), in an alkali capture reaction during the release of chlorine as HCl to the gas phase.

## 6 The measurement campaign in Munksund

The results from the full-scale measurement campaign are presented separately from the results obtained at Chalmers. This measurement campaign is an example of how the strategies discussed in the previous chapters can be applied in a full-scale CFB boiler.

### 6.1 Results from the short-term measurements

Fig. 6.1 shows a comparison of KCl and SO<sub>2</sub> obtained from IACM for test cases Peat Ref and AS. KCl was lowered from approximately 17 ppm during normal fuel mix to less than 2 ppm for AS. Only a minor decrease in KCl was observed during test case Peat compared to Ref. Fig. 6.2 shows alkali (Na + K), Cl and S expressed as mole % in deposits collected at 500°C during test cases Peat, Ref and AS. Deposits collected during test case Ref had a rather high content of both alkali and chlorine yet low of sulphur. They contained more sulphur and less chlorine during test case Peat. The deposits from AS had an even higher content of sulphur than from Peat, and no detectable amounts of chlorine were found. Peat performed significantly better in lowering chlorine in the deposit than reducing KCl in the gas phase. This indicated chlorine was lowered by either an alkali capture mechanism or by heterogeneous sulphation of the alkali in the deposit.

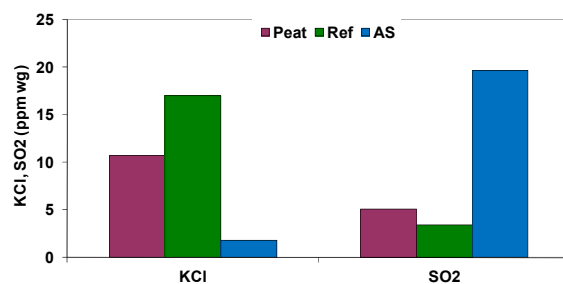


**Fig. 6.1.** KCl and SO<sub>2</sub> obtained from IACM during test cases Peat, Ref and AS. wg = wet flue gas.

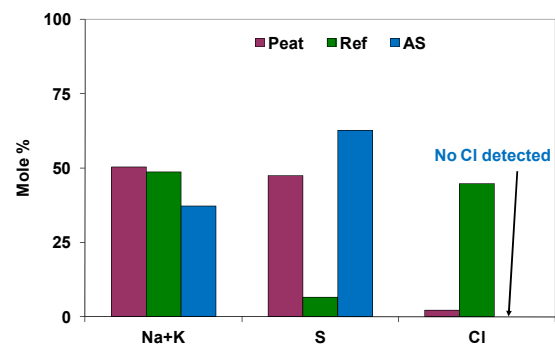


**Fig. 6.2.** Na + K, Cl, and S expressed as mole % in deposits collected at 500°C during test cases Peat, Ref, and AS. No Cl was detected during AS.

Results from impactor measurements during Ref and AS revealed the finest particles consisted mainly of K and Cl originating from gaseous KCl during Ref. Only a minor amount of Cl was detected during AS whereas sulphur increased. This is a further indication that sulphation of gaseous KCl occurred during AS. The interpretation of the results for test case Peat was considerably more complex. Impactor measurements for Peat were performed during a so-called pre-test and only a few stages from it were

analysed. The composition of the stages with the finest particles for Peat is compared with the same stage for Ref and AS in Fig. 6.3. The finest particles consisted mainly of K, Na and Cl originating from gaseous KCl and NaCl during both Ref and Peat. Only a minor amount of Cl was detected during AS and sulphur increased instead. The high content of Cl for Peat is in agreement with the results concerning gas phase alkali chlorides obtained from IACM in Fig. 6.1. Homogeneous sulphation of gaseous KCl was thus less relevant during co-combustion of peat.

The demonstration and evaluation of measures to reduce alkali related problems in a full-scale boiler is a major challenge. Several precautions were taken to compensate for the greater risk of experimental deviations. The use of independent measurement tools in combination with an overall judgement of the relevance of each result was believed to be sufficient to make an appropriate interpretation. The overall results concerning AS were consistent and an efficient sulphation of gaseous KCl indicated the importance of SO<sub>3</sub>. The results from IACM were supported by decreased Cl in the finest particles collected by the impactor. Furthermore deposits collected contained less Cl and more S in comparison with Ref. Peat performed significantly better in lowering Cl in the deposit than reducing KCl in the gas phase. This indicated chlorine was lowered by either an alkali capture mechanism or by heterogeneous sulphation of the alkali in the deposit. To a certain extent, the results were contradictory and it remains unclear whether the chlorine in the deposits was decreased due to sulphation or due to alkali capture for test case Peat.

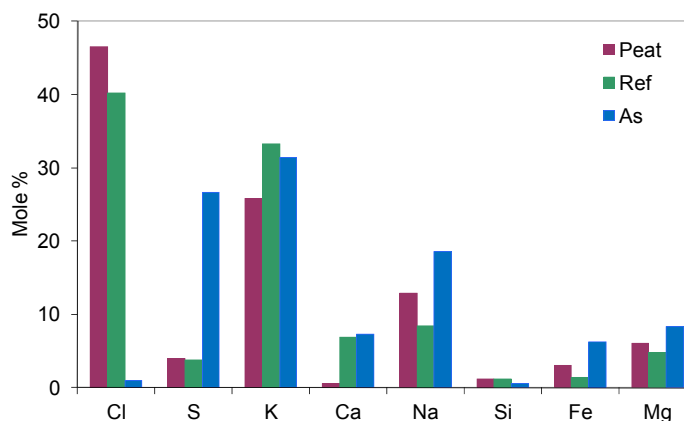


**Fig. 6.3.** Relative elemental compositions in mole % for the finest particles (<0.03µm) collected by the impactor during Ref, AS and Peat.

## 6.2 Results from the long-term measurements

The concept with parallel cyclones enabled the performance of a four-week measurement campaign with two identical corrosion probes exposed on either side of the boiler, but with ammonium sulphate (AS) injection in one of the cyclones and using the other one as a reference. The photographs in Fig. 6.4 illustrate that AS had a great impact on both the formation and the appearance of the deposits.





**Fig. 6.4a.** Deposits on the corrosion probe rings after four weeks' exposure with normal fuel mix (test case Ref).



**Fig. 6.4b.** Deposits on the corrosion probe rings after four weeks' exposure with normal fuel mix and injection of ammonium sulphate (test case AS).

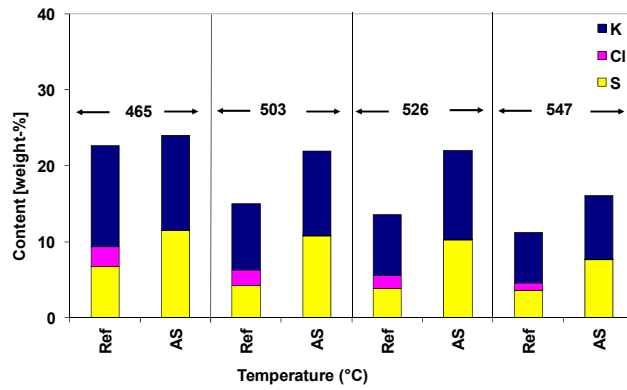


**Fig. 6.5.** K, Cl, S on deposits after four weeks' exposure on corrosion probe rings made of 13CrMo44.

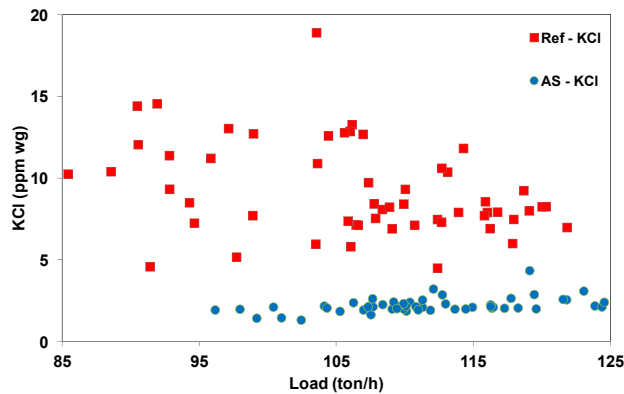


**Fig. 6.6.** Daily averages of KCl as a function of boiler load with and without injection of AS.

Wet chemical analysis was performed on deposits collected at temperatures ranging from 465 to 547°C on test rings 3, 6, 9 and 14 made of 13CrMo44. It is a commonly used low alloyed superheater material and SH2 was also made of 13CrMo44. Fig. 6.5 showed that

Cl was present in the deposits during Ref and no Cl was found during AS over the whole temperature range. This was consistent with the results from short-term exposure and confirmed that AS reduces chlorine and increases sulphur in deposits also during longer times of exposure.

The ten-week corrosion measurement was carried out with injection of AS controlled towards a fixed level of gaseous KCl by means of IACM. Fig. 6.6 shows daily averages of KCl as a function of boiler load with injection of AS compared to a reference period with normal fuel mix (Ref) and no injection. The level of KCl varied significantly from one measurement day to the next during Ref due to changes in the chlorine content in the in-coming fuel mix. Despite these variations, it was possible to maintain a fixed level of approximately 2 ppm KCl by controlling the flow of AS by IACM. The corrosion rates obtained were evaluated and are presented in Fig. 6.7 for Ref and AS during a four-week measurement campaign and also during a ten-week measurement for AS. Trends were observed both concerning temperature and choice of material and typically the corrosion rate during AS was 20 – 50 % in comparison with normal conditions (Ref).

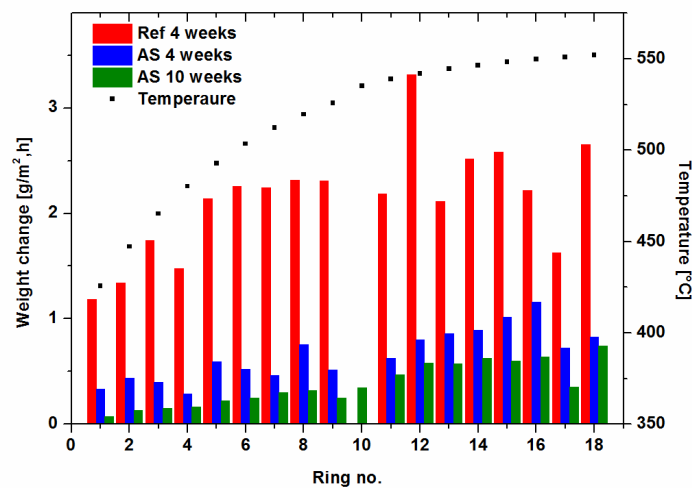


**Fig. 6.7.** Corrosion rates during a four week measurement for Ref and AS and during a ten week measurement for AS. The exposed ring materials are shown in Fig. 3.5.

## 7 Conclusions

### 7.1 Importance of SO<sub>2</sub> and SO<sub>3</sub> for sulphation of gaseous KCl

The performance of elemental sulphur (S) and ammonium sulphate (AS) for sulphation of gaseous KCl was evaluated in Paper I. The sulphation was more efficient with AS even when the S/Cl molar ratio was less than half compared to sulphur. Thus the presence of gaseous SO<sub>3</sub> is of greater importance than that of SO<sub>2</sub> for the sulphation of gaseous KCl.

The sulphation of gaseous KCl was investigated during injection of ammonium sulphate for three air excess ratios ( $\lambda = 1.1, 1.2$  and  $1.4$ ). AS was injected at three positions: in the upper part of the combustion chamber, in the cyclone inlet and in the hot cyclone. Two experimental procedures were applied focusing on the effect of combustibles and oxygen. The main conclusions are summarised below:

- The injection point for AS in the upper part of the combustion chamber at the lowest air excess ratio ( $\lambda = 1.1$ ) had the highest concentrations of combustibles. The poorest sulphation of gaseous KCl was attained in this location and it was explained by the fact that SO<sub>3</sub> was partly consumed by side reactions due to the presence of combustibles.
- The injection point for AS with the best performance for sulphation of KCl was in the cyclone during the highest air excess ratio ( $\lambda = 1.4$ ). Here the formation of SO<sub>2</sub> from SO<sub>3</sub> and the consumption of SO<sub>3</sub> from side reactions were minimised.
- The position in the boiler had a great impact on the sulphation of gaseous KCl when injecting AS at different air excess ratios. The optimal position and conditions can be identified by measuring KCl with IACM with and without injection of AS.
- Less gaseous KCl was reduced when injecting AS in the cyclone during the lowest air excess ratio compared to the higher ratios. The highest content of chlorine was found in the deposits without injection of AS. Significant amounts of chlorine were still present during injection of AS at a molar ratio S/Cl of 1.4 at  $\lambda = 1.1$ . No Cl was detected in the deposits at an S/Cl of only 1.3 at  $\lambda = 1.4$ .
- A correlation was observed between the sulphation of gaseous KCl and reduced chlorine content in the deposits when injecting AS. This suggests measurements of KCl by IACM can give an indication of the risk for increased chlorine content in the deposits during operation of a full-scale boiler.
- Calculations using a chemical kinetic model supported that the presence of volatile combustibles could have an impact on the sulphation of gaseous KCl.

## 7.2 Co-combustion and ammonium sulphate

Two strategies were evaluated to decrease the risk of superheater corrosion by reducing gaseous KCl and content of chlorine in deposits during biomass combustion. These strategies were co-combustion with peat and injection of ammonium sulphate. The main conclusions are summarised below:

- The overall performance was somewhat better for ammonium sulphate which significantly reduced gaseous KCl and no chlorine was found in the deposits.
- Although the reduction of gaseous KCl was less efficient during co-combustion with peat, the chlorine content in the deposits was, nevertheless, greatly reduced.
- The reduction of chlorine in the deposits was allegedly due to capture of potassium by reactive components from the peat ash (Al, Fe, Ca and/or Si) in parallel to sulphation of KCl during co-combustion with peat. These compounds remained unidentified.

## 7.3 Suggestions for future work

This work has mainly focused on strategies to reduce gaseous KCl and chlorine in deposits during combustion of biomass in CFB boilers. The correlation between concentration of gaseous KCl, the content of chlorine in deposits and superheater corrosion needs to be further investigated.

It was suggested that chlorine in the deposits was reduced due to capture of potassium by reactive components from the peat ash in parallel to sulphation of KCl during co-combustion with peat. These compounds remained unidentified and further investigations are necessary.

The performance of elemental sulphur and ammonium sulphate was mainly evaluated for sulphation of gaseous KCl and chlorine in deposits. These additives have an impact on the emission of other compounds as well. Their impact on SNCR chemistry and CO can be a part of a future investigation.

The kinetic model overestimated the SO<sub>2</sub> sulphation capacity by a pathway that bypassed SO<sub>3</sub>. This pathway favoured sulphation of KCl in the presence of combustibles to almost the same levels as the SO<sub>3</sub> pathway. The experimental result, however, indicates a higher influence of combustibles. This requires further investigations.

The nitrogen chemistry could be included in future calculations in the chemical kinetic model to study any interactions from the ammonium part of AS. The calculations presented were only performed at a specific temperature and it is suggested to study sulphation over a wider temperature range.

## 8 References

- [1] J. Werkelin, Ash-forming elements and their chemical forms in woody biomass fuels, in: Process Chemistry Centre, PhD, Åbo Akademi, 2008.
- [2] S. C. van Lith, V. Alonso-Ramirez, P. A. Jensen, F. J. Frandsen, P. Glarborg, Release to the gas phase of inorganic elements during wood combustion. Part 1: Development and evaluation of quantification methods, *Energy Fuels* 20 (2006) 964-978.
- [3] J. N. Knudsen, P. A. Jensen, K. Dam-Johansen, Transformation and release to the gas phase of Cl, K, and S during combustion of annual biomass, *Energy Fuels* 18 (2004) 1385-1399.
- [4] H. M. Westberg, M. Byström, B. Leckner, Distribution of potassium, chlorine, and sulfur between solid and vapor phases during combustion of wood chips and coal, *Energy Fuels* 17 (2003) 18-28.
- [5] L. L. Baxter, T. R. Miles, B. M. Jenkins, T. Milne, D. Dayton, R. W. Bryers, L. L. Oden, The behavior of inorganic material in biomass-fired power boilers: field and laboratory experiences, *Fuel Process. Technol.* 54 (1998) 47-78.
- [6] K. A. Christensen, M. Stenholm, H. Livbjerg, The formation of submicron aerosol particles, HCl and SO<sub>2</sub> in straw-fired boilers, *J. Aerosol Sci* 29 (1998) 421-444.
- [7] M. Theis, B. J. Skrifvars, M. Zevenhoven, M. Hupa, H. H. Tran, Fouling tendency of ash resulting from burning mixtures of biofuels. Part 2: Deposit chemistry, *Fuel* 85 (2006) 1992-2001.
- [8] H. P. Nielsen, F. J. Frandsen, K. Dam-Johansen, L. L. Baxter, The implications of chlorine-associated corrosion on the operation of biomass-fired boilers, *Prog. Energy Combust. Sci.* 26 (2000) 283-298.
- [9] S. C. van Lith, F. J. Frandsen, M. Montgomery, T. Vilhelmsen, S. A. Jensen, Lab-scale Investigation of Deposit-induced Chlorine Corrosion of Superheater Materials under Simulated Biomass-firing Conditions. Part 1: Exposure at 560 degrees C, *Energy Fuels* 23 (2009) 3457-3468.
- [10] H. Kassman, C. Andersson, J. Högberg, L.-E. Åmand, K. Davidsson, Gas phase alkali chlorides and deposits during Co-combustion of coal and biomass, 19th International Conference on Fluidized Bed Combustion, Vienna, Austria, 2006.
- [11] K. Davidsson, L.-E. Åmand, H. Kassman, E. Edvardsson, J. Högberg, On-line measurement of alkali chlorides during co-combustion of coal and biomass, in: 15th European Biomass Conference & Exhibition, Berlin, Germany, 2007.
- [12] M. Öhman, A. Nordin, B. J. Skrifvars, R. Backman, M. Hupa, Bed agglomeration characteristics during fluidized bed combustion of biomass fuels, *Energy Fuels* 14 (2000) 169-178.
- [13] A. A. Khan, W. de Jong, P. J. Jansens, H. Spliethoff, Biomass combustion in fluidized bed boilers: Potential problems and remedies, *Fuel Process. Technol.* 90 (2009) 21-50.
- [14] E. Brus, M. Öhman, A. Nordin, Mechanisms of bed agglomeration during fluidized-bed combustion of biomass fuels, *Energy Fuels* 19 (2005) 825-832.

- [15] A. Zbogar, F. Frandsen, P. A. Jensen, P. Glarborg, Shedding of ash deposits, *Prog. Energy Combust. Sci.* 35 (2009) 31-56.
- [16] M. Aho, E. Ferrer, Importance of coal ash composition in protecting the boiler against chlorine deposition during combustion of chlorine-rich biomass, *Fuel* 84 (2005) 201-212.
- [17] A. L. Elled, K. O. Davidsson, L.-E. Åmand, Sewage sludge as a deposit inhibitor when co-fired with high potassium fuels, *Biomass Bioenergy* 34 (2010) 1546-1554.
- [18] R. A. Khalil, E. Housfar, W. Musinguzi, M. Becidan, Ø. Skreiberg, F. Goile, T. Løvås, L. Sørum, Experimental Investigation on Corrosion Abatement in straw Combustion by Fuel Mixing, *Energy Fuels* 25 (2011) 2687-2695.
- [19] K. O. Davidsson, L. E. Åmand, B. M. Steenari, A. L. Elled, D. Eskilsson, B. Leckner, Countermeasures against alkali-related problems during combustion of biomass in a circulating fluidized bed boiler, *Chem. Eng. Sci.* 63 (2008) 5314-5329.
- [20] K. Lundholm, A. Nordin, M. Öhman, D. Boström, Reduced Bed Agglomeration by Co-combustion Biomass with Peat Fuels in a Fluidized Bed, *Energy Fuels* 19 (2005) 2273-2278.
- [21] L. Pommer, M. Öhman, D. Boström, J. Burvall, R. Backman, I. Olofsson, A. Nordin, Mechanisms Behind the Positive Effects on Bed Agglomeration and Deposit Formation Combusting Forest Residue with Peat Additives in Fluidized Beds, *Energy Fuels* 23 (2009) 4245-4253.
- [22] P. Yrjas, B. J. Skrifvars, M. Hupa, J. Roppo, M. Nylund, P. Vainikka, Chlorine in deposits during co-firing of biomass, peat, and coal in a full-scale CFBC boiler, *Proceedings of the 18th International Conference on Fluidized Bed Combustion*, Toronto, Canada, 2005, pp. 679-687.
- [23] K. O. Davidsson, L.-E. Åmand, A. L. Elled, B. Leckner, Effect of cofiring coal and biofuel with sewage sludge on alkali problems in a circulating fluidized bed boiler, *Energy Fuels* 21 (2007) 3180-3188.
- [24] M. Aho, A. Gil, R. Taipale, P. Vainikka, H. Vesala, A pilot-scale fireside deposit study of co-firing Cynara with two coals in a fluidised bed, *Fuel* 87 (2008) 58-69.
- [25] A. Pettersson, A. L. Elled, A. Möller, B. M. Steenari, L. E. Åmand, The impact of zeolites during co-combustion of municipal sewage sludge with alkali and chlorine rich fuels, *Proceedings of the 20th International Conference on Fluidized Bed Combustion*, 2009, pp. 902-909.
- [26] B. M. Steenari, O. Lindqvist, High-temperature reactions of straw ash and the anti-sintering additives kaolin and dolomite, *Biomass Bioenergy* 14 (1998) 67-76.
- [27] K. Q. Tran, K. Iisa, B. M. Steenari, O. Lindqvist, A kinetic study of gaseous alkali capture by kaolin in the fixed bed reactor equipped with an alkali detector, *Fuel* 84 (2005) 169-175.
- [28] M. Öhman, A. Nordin, The role of kaolin in prevention of bed agglomeration during fluidized bed combustion of biomass fuels, *Energy Fuels* 14 (2000) 618-624.
- [29] M. Aho, J. Silvennoinen, Preventing chlorine deposition on heat transfer surfaces with aluminium-silicon rich biomass residue and additive, *Fuel* 83 (2004) 1299-1305.
- [30] S. Q. Turn, C. M. Kinoshita, D. M. Ishimura, J. Zhou, T. T. Hiraki, S. M. Masutani, A review of sorbent materials for fixed bed alkali getter systems in biomass gasifier combined cycle power generation applications, *Journal of the Institute of Energy* 71 (1998) 163-177.

- [31] H. J. Grabke, E. Reese, M. Spiegel, The effects of chlorides, hydrogen chloride, and sulfur dioxide in the oxidation of steels below deposits, *Corros. Sci.* 37 (1995) 1023-1043.
- [32] J. Pettersson, H. Asteman, J.-E. Svensson, L.-G. Johansson, KCl Induced Corrosion of a 304-type Austenitic Stainless Steel at 600°C; The Role of Potassium, *Oxid. Met.* 64 (2005) 23-41.
- [33] N. Folkesson, T. Jonsson, M. Halvarsson, L.-G. Johansson, J.-E. Svensson, The influence of small amounts of KCl(s) on the high temperature corrosion of a Fe-2.25Cr-1Mo steel at 400 and 500°C., *Materials and Corrosion*. In Press, doi: 10.1002/maco.201005942 (2010).
- [34] J. Pettersson, C. Pettersson, N. Folkesson, L.-G. Johansson, E. Skog, J.-E. Svensson, The influence of sulphur additions on the corrosive environment in a waste-fired CFB boiler, *Mater. Sci. Forum* 522-523 (2006) 563-570.
- [35] N. Folkesson, J. Pettersson, C. Pettersson, L.-G. Johansson, E. Skog, J.-E. Svensson, Fireside corrosion of stainless and low alloyed steels in a waste-fired CFB boiler; The effect of adding sulphur to the fuel *Mater. Sci. Forum* 595-598 (2008) 289-297.
- [36] B. J. Skrifvars, R. Backman, M. Hupa, K. Salmenoja, E. Vakkilainen, Corrosion of superheater steel materials under alkali salt deposits Part 1: The effect of salt deposit composition and temperature, *Corros. Sci.* 50 (2008) 1274-1282.
- [37] B. J. Skrifvars, M. Westén-Karlsson, M. Hupa, K. Salmenoja, Corrosion of superheater steel materials under alkali salt deposits. Part 2: SEM analyses of different steel materials, *Corros. Sci.* 52 (2010) 1011-1019.
- [38] J. Pettersson, J. E. Svensson, L. G. Johansson, Alkali Induced Corrosion of 304-type Austenitic Stainless Steel at 600 degrees C; Comparison between KCl, K<sub>2</sub>CO<sub>3</sub> and K<sub>2</sub>SO<sub>4</sub>, *High Temperature Corrosion and Protection of Materials* 7, Pts 1 and 2 595-598 (2008) 367-375.
- [39] P. Henderson, C. Andersson, H. Kassman, The use of fuel additives in wood and waste wood-fired boilers to reduce corrosion and fouling problems, *VGB PowerTech* 84 (2004) 58-62.
- [40] M. Broström, H. Kassman, A. Helgesson, M. Berg, C. Andersson, R. Backman, A. Nordin, Sulfation of corrosive alkali chlorides by ammonium sulfate in a biomass fired CFB boiler, *Fuel Process. Technol.* 88 (2007) 1171-1177.
- [41] H. Kassman, M. Holmgren, E. Edvardsson, L.-E. Åmand, J. Öhlin, Nitrogen containing additives for simultaneous reduction of KCl and NO<sub>x</sub> during biomass combustion in a CFB boiler, 9th International Conference on Circulating Fluidized Beds, Hamburg, Germany, 2008.
- [42] J. H. Zeuthen, P. A. Jensen, J. P. Jensen, H. Livbjerg, Aerosol formation during the combustion of straw with addition of sorbents, *Energy Fuels* 21 (2007) 699-709.
- [43] P. Glarborg, Hidden interactions - Trace species governing combustion and emissions, *Proceedings of the Combustion Institute* 31 (2007) 77-98.
- [44] J. R. Jensen, L. B. Nielsen, C. Schultz-Møller, S. Wedel, H. Livbjerg, The nucleation of aerosols in flue gases with a high content of alkali - A laboratory study, *Aerosol Science and Technology* 33 (2000) 490-509.
- [45] K. O. Davidsson, L.-E. Åmand, B. Leckner, B. Kovacevik, M. Svane, M. Hagström, J. B. C. Pettersson, J. Petterson, H. Asteman, J.-E. Svensson, L. G. Johansson, Potassium,

chlorine, and sulfur in ash, particles, deposits, and corrosion during wood combustion in a circulating fluidized-bed boiler, *Energy Fuels* 21 (2007) 71-81.

[46] K. Iisa, Y. Lu, K. Salmenoja, Sulfation of potassium chloride at combustion conditions, *Energy Fuels* 13 (1999) 1184-1190.

[47] S. Jimenez, J. Ballester, Effect of co-firing on the properties of submicron aerosols from biomass combustion, *Proceedings of the Combustion Institute* 30 (2005) 2965-2972.

[48] S. Jimenez, J. Ballester, Formation of alkali sulphate aerosols in biomass combustion, *Fuel* 86 (2007) 486-493.

[49] L. Hindiyarti, F. Frandsen, H. Livbjerg, P. Glarborg, P. Marshall, An exploratory study of alkali sulfate aerosol formation during biomass combustion, *Fuel* 87 (2008) 1591-1600.

[50] P. Glarborg, P. Marshall, Mechanism and modeling of the formation of gaseous alkali sulfates, *Combust. Flame* 141 (2005) 22-39.

[51] M. Steinberg, K. Schofield, The controlling chemistry of surface deposition from sodium and potassium seeded flames free of sulfur or chlorine impurities, *Combust. Flame* 129 (2002) 453-470.

[52] L. Boonsongsup, K. Iisa, W. J. Frederick Jr, Kinetics of the Sulfation of NaCl at Combustion Conditions, *Ind. Eng. Chem. Res.* 36 (1997) 4212-4216.

[53] L. Hindiyarti, Gas phase sulphur, chlorine, potassium chemistry in biomass combustion, in: DTU, PhD, Technical University of Denmark, 2007.

[54] L. Hindiyarti, P. Glarborg, P. Marshall, Reactions of SO<sub>3</sub> with the O/H radical pool under combustion conditions, *J. Phys. Chem. A* 111 (2007) 3984-3991.

[55] L. Hindiyarti, F. Frandsen, H. Livbjerg, P. Glarborg, Influence of potassium chloride on moist CO oxidation under reducing conditions: Experimental and kinetic modeling study, *Fuel* 85 (2006) 978-988.

[56] C. K. Westbrook, F. L. Dryer, Chemical kinetic modeling of hydrocarbon combustion, *Prog. Energy Combust. Sci.* 10 (1984) 1 - 57.

[57] M. Becidan, L. Sørum, F. Frandsen, A. Juul Pedersen, Corrosion in waste-fired boilers: a thermodynamic study, *Fuel* 88 (2009) 595-604.

[58] M. P. Glazer, N. A. Khan, W. de Jong, H. Spliethoff, H. Schürmann, P. Monkhouse, Alkali Metals in Circulating Fluidized Bed Combustion of Biomass and Coal: Measurements and Chemical Equilibrium Analysis, *Energy Fuels* 19 (2005) 1889-1897.

[59] J. M. Johansen, J. G. Jakobsen, F. J. Frandsen, P. Glarborg, Release of K, Cl, and S during Pyrolysis and Combustion of High-Chlorine Biomass, *Energy Fuels* 25 (2011) 4961-4971.

[60] M. Becidan, E. Housfar, R. A. Khalil, Ø. Skreiberg, T. Løvås, L. Sørum, Optimal mixtures to reduce formation of corrosive compounds during straw combustion: A thermodynamic Analysis, *Energy Fuels* 25 (2011) 3223-3234.

[61] C. L. Rasmussen, P. Glarborg, P. Marshall, Mechanisms of radical removal by SO<sub>2</sub>, *Proceedings of the Combustion Institute* 31 (2007) 339-347.

[62] A. Yilmaz, L. Hindiyarti, A. D. Jensen, P. Glarborg, P. Marshall, Thermal dissociation of SO<sub>3</sub> at 1000-1400K, *J. Phys. Chem. A* 110 (2006) 6654-6659.

[63] R. Heikkinen, R. S. Laitinen, T. Patrikainen, M. Tiainen, M. Virtanen, Slagging tendency of peat ash, *Fuel Process. Technol.* 56 (1998) 69-80.



- [64] L. Tobiasen, R. Skytte, L. S. Pedersen, S. T. Pedersen, M. A. Lindberg, Deposit characteristic after injection of additives to a Danish straw-fired suspension boiler, *Fuel Process. Technol.* 88 (2007) 1108-1117.
- [65] E. Lindström, M. Sandström, D. Boström, M. Öhman, Slagging Characteristics during Combustion of Cereal Grains Rich in Phosphorus, *Energy Fuels* 21 (2007) 710-717.
- [66] X. Wei, U. Schnell, K. R. G. Hein, Behaviour of gaseous chlorine and alkali metals during biomass thermal utilisation, *Fuel* 84 (2005) 841-848.
- [67] K. Salmenoja, Field and laboratory studies on chlorine-induced superheater corrosion in boilers fired with biofuels, in: Department of Chemical Engineering, PH.D. Thesis, Åbo Akademi University, 2000.
- [68] C. Forsberg, M. Broström, R. Backman, E. Edvardsson, S. Badiei, M. Berg, H. Kassman, Principle, calibration, and application of the in situ alkali chloride monitor, *Rev. Sci. Instrum.* 80 (2009).
- [69] European Patent EP 1221036 (2006).
- [70] European Patent EP 1354167 (2006).
- [71] L. S. Bäfver, Particles from biomass combustion - characterisation and influence of additives, in: Dep. Energy & Environment, PhD, Chalmers University of Technology, 2008.
- [72] E. Vainio, P. Yrjas, M. Zevenhoven, A. Brink, T. Laurén, M. Hupa, The fate of chlorine, sulfur and potassium during co-combustion of bark, sludge and REF in a 107MW<sub>th</sub> BFB boiler, *Impacts of Fuel Quality*, Lapland, Finland, 2010.
- [73] F. J. Frandsen, Ash formation, deposition and corrosion when utilizing straw for heat and power production, in: DTU Chemical Engineering, Publishable Doctoral Thesis, Technical University of Denmark, 2011.
- [74] M. Broström, Aspects of alkali chloride chemistry on deposit formation and high temperature corrosion in biomass and waste fired boilers, in: *Energy Technology and Thermal Process Chemistry*, PhD, Umeå University, 2010.
- [75] B. Leckner, M. Karlsson, K. Dam-Johansen, C. E. Weinell, P. Kilpinen, M. Hupa, Influence of additives on selective noncatalytic reduction of NO with NH<sub>3</sub> in circulating fluidized bed boilers, *Ind. Eng. Chem. Res.* 30 (1991) 2396-2404.
- [76] L. Gustavsson, P. Glarborg, B. Leckner, Modelling of chemical reactions in afterburning for the reduction of N<sub>2</sub>O, *Combust. Flame* 106 (1996) 345-358.
- [77] P. Viklund, H. Kassman, L. E. Åmand, Deposit chemistry and initial corrosion - The influence of excess O<sub>2</sub> and sulphate injection, (2012) In manuscript.

